ISSN 0252-1075

# IITM TECHNICAL REPORT [TR-09]

ESSO/IITM/CCCR/TR/02(2025)/204

# IITM-Hydrometeorological Observation System: Scalable climate monitoring with Internet of Things

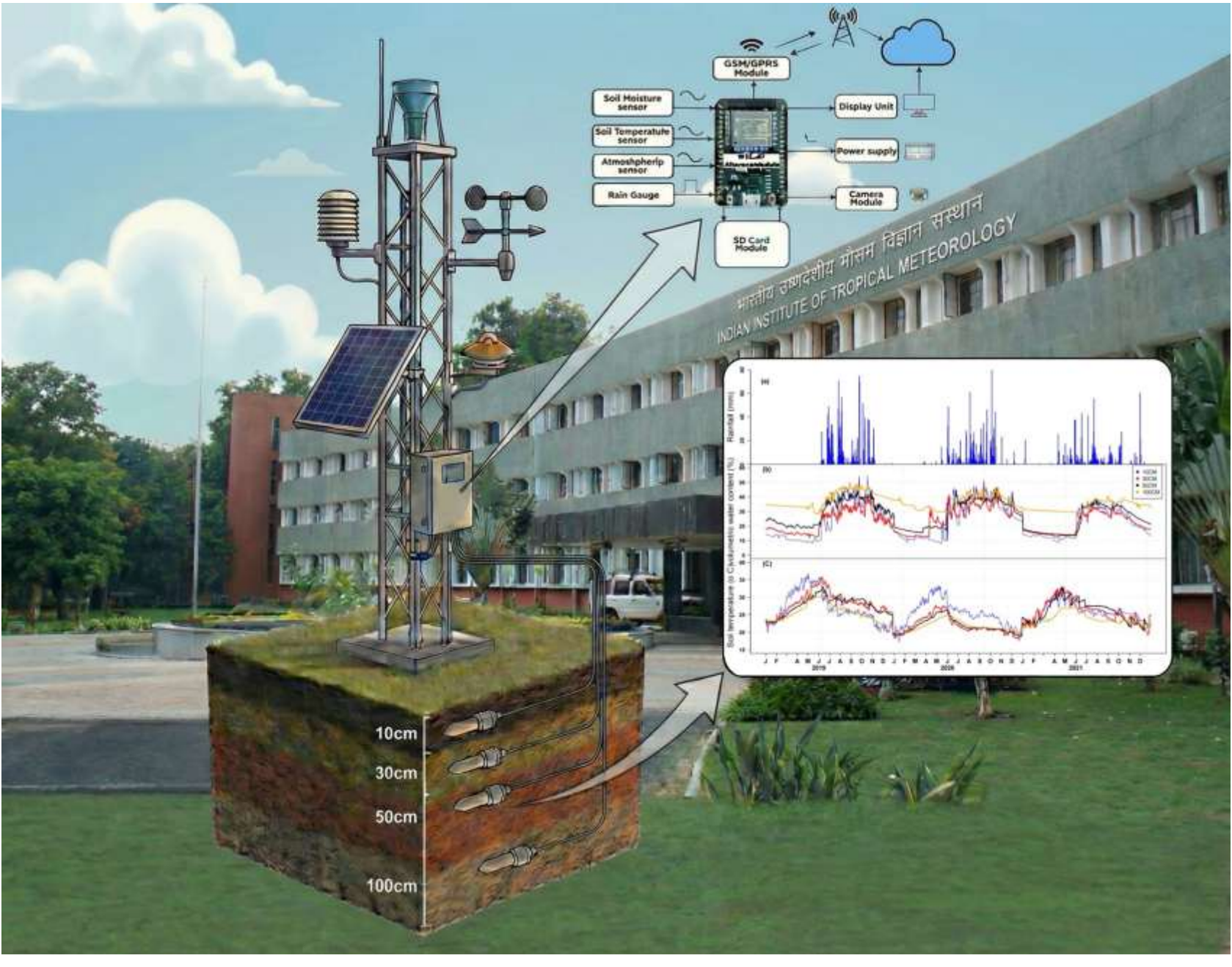


**Mangesh Mohanrao Goswami, Bhupendra Bahadur Singh, Madhusudan Ingale, Naresh Ganeshi, Aju CD, Amey Datye, Manish Ranalkar, Milind Mujumdar, and R Krishnan**

Indian Institute of Tropical Meteorology (IITM)
Ministry of Earth Sciences (MoES)
Pune-411008, Maharashtra, India
https://www.tropmet.res.in/

**ISSN 0252-1075**
**Contribution from IITM**
**Technical Report No. TR-09**
**ESSO/IITM/CCCR/TR/02(2025)/204**

# IITM-Hydrometeorological Observation System: Scalable climate monitoring with Internet of Things

Mangesh Mohanrao Goswami[1*], Bhupendra Bahadur Singh[1*], Madhusudan Ingale[1], Naresh Ganeshi[1], Aju CD[1], Amey Datye[1], Manish Ranalkar[2], Milind Mujumdar[1], and R Krishnan[1]

[1]Indian Indian Institute of Tropical Meteorology (Ministry of Earth Sciences), Pune-411008, Maharashtra, India

[2]India Meteorological Department (IMD), Regional Meteorological Centre, Lucknow-226009, Uttar Pradesh, India

***Corresponding Authors:**

Dr. Mangesh Mohanrao Goswami
(Project Scientist-II),
Centre for Climate Change Research,
Indian Institute of Tropical Meteorology,
Dr. Himi Bhabha Road, Pashan, Pune 411 008,
Maharashtra, India
Email: mangesh@tropmet.res.in

Dr. Bhupendra Bahadur Singh
(Scientist-E)
Centre for Climate Change Research,
Indian Institute of Tropical Meteorology,
Dr. Himi Bhabha Road, Pashan, Pune 411108,
Maharashtra, India
Email: bhupendra.cat@tropmet.res.in

Indian Institute of Tropical Meteorology (IITM)
Ministry of Earth Sciences (MoES)
Pune-411008, Maharashtra, India
https://www.tropmet.res.in/

# DOCUMENT CONTROL SHEET

---

**Ministry of Earth Sciences (MoES)**
**Indian Institute of Tropical Meteorology (IITM)**

**ESSO Document Number**
ESSO/IITM/CCCR/TR/02(2025)/204

**Title of the Report**
IITM-Hydrometeorological Observation System: Scalable climate monitoring with Internet of Things

**Authors**
Mangesh Mohanrao Goswami, Bhupendra Bahadur Singh, Madhusudan Ingale, Naresh Ganeshi, Aju CD, Amey Datye, Manish Ranalkar, Milind Mujumdar, and R Krishnan

**Reviewers**
Prof. Prashant K Srivastava
[Institute of Environment & Sustainable Development, Banaras Hindu University, Varanasi]
Dr. N. R. Patel
[Head, Agriculture and Soils Department, Indian Institute of Remote Sensing, Dehradun]

**Type of Document**
Technical Report

**Number of pages and figures**
44, 20

**Number of references**
37

**Keywords**
Soil moisture, Soil temperature, Gravimetric observations, ESP32, Phenocam, COSMOS

**Security classification**
Open

**Distribution**
Unrestricted

**Date of Publication**
December 2025

# Abstract

Conventional soil moisture (SM) measurements rely on manual methods, limiting coverage and resolution. This report describes an IoT-based hydro-meteorological monitoring system deployed at the IITM-COSMOS site since 2019, enabling automated, real-time, and cost-effective measurements of SM, soil temperature, air temperature, humidity, pressure, and phenological records. The system integrates multiple sensors, low-energy Bluetooth communication, email and SMS alerts, dual solar-battery power, and sensor-damage notifications. Its high-resolution, real-time data, overcome limitations of conventional methods, offering a scalable and modular solution for climate research, resource management, and agricultural applications.

# Summary

This report presents the development of an IoT-based hydro-meteorological monitoring system to address the need for accurate soil moisture and climate observations. The system supports advancements in weather and climate science, land-atmosphere interaction studies, and agricultural management. It was developed and deployed at the IITM-COSMOS site in Pune, India, and its performance is evaluated against standard observations. The system provides real-time, automated observations of soil moisture, soil temperature, air temperature, humidity, pressure, rainfall, and phenological data. A modular architecture based on ESP32 microcontrollers enables flexible sensor integration and scalability. Multiple communication technologies, including BLE, GSM/GPRS, and Wi-Fi, ensure reliable data transmission. Dual power sources (solar and battery) support uninterrupted, long-term operation. Area-averaged, multi-depth measurements improve representativeness compared to traditional point-based methods. Features such as sensor-damage alerts and auger-assisted deployment enhance data quality and system reliability. The system has also been utilized for training and demonstration purposes, with the objective of equipping diverse stakeholders with first-hand knowledge of soil hydro-meteorological processes, thereby facilitating its potential adoption and practical application. Overall, the system offers a cost-effective solution with strong potential for climate-resilient agriculture, water management, and environmental research.

# List of Acronyms and Symbols

| | |
|---|---|
| **AT** | Attention commands |
| **BLE** | Bluetooth Low energy |
| **BME680** | Bosch Sensortec |
| **CPU** | Central Processing Unit |
| **EEPROM** | Electrically Erasable Programmable Read-only Memory |
| **ESP32** | Espressif System-on-Chip |
| **GPIO** | General Purpose Input / Output |
| **GSM** | Global System for Mobile Communications |
| **HTTP** | Hyper-Text Transfer Protocol |
| **HVAC** | Heat, Ventilation, and Air Conditioning |
| **I2C** | Inter-Integrated Circuit |
| **IITM** | Indian Institute of Tropical Meteorology |
| **IMD** | Indian Meteorology Department |
| **IoT** | Internet of Things |
| **KBC-NMU** | Kavayitri Bahinabai Chaudhari North Maharashtra University |
| **LCD** | Liquid Crystal Display |
| **MCU** | Main Controlling Unit |
| **MoES** | Ministry of Earth Sciences |
| **NWP** | Numerical Weather Prediction |
| **PCB** | Printed Circuit Board |
| **RMSE** | Root Mean Square Error |
| **Rx** | Receiver |
| **SCK** | Serial Clock |
| **SDA** | Serial Data |
| **SDI-12** | Serial/Digital Interface at 1200 baud |
| **SIM** | Subscriber Identity Module |
| **SM** | Soil moisture |
| **SMS** | Short Message Service |
| **SMTP** | Simple Mail Transfer Protocol |
| **SPI** | Serial Peripheral Interface |
| **ST** | Soil temperature |
| **STD** | Standard deviation |
| **TBR** | Tipping Bucket Rain gauge |
| **TDR** | Time-Domain Reflectometry |
| **TFT** | Thin-Film-Transistor |
| **Tx** | Transmitter |
| **UART** | Universal Asynchronous Receiver/Transmitter |
| **UbRMSE** | Unbiased Root Mean Square Error |
| **VWC** | Volumetric Water Content |
| **WIFI** | Wireless Fidelity |

| | |
|---|---|
| $M_{dry}$ | Mass of Dry soil |
| $M_{wet}$ | Mass of wet soil |
| $\theta_g$ | Gravimetric soil moisture content |
| $\rho_b$ | Bulk density of the soil |
| $\rho_w$ | Density of water |

# List of Figures

# List of Tables

# Table of Contents

# Acknowledgement

The authors gratefully acknowledge the invaluable support and guidance received from various individuals and institutions towards the development of this Hydrometeorological observation system. We extend our sincere thanks to the Director, Indian Institute of Tropical Meteorology (IITM), and the Secretary, Ministry of Earth Sciences (MoES), Government of India, for providing the institutional framework, infrastructure, and encouragement that made this work possible. We also express our deep appreciation to the Project Director, Centre for Climate Change Research (CCCR) at IITM for extending continued support.

Our heartfelt gratitude goes to Dr. Dharmaraj for his insightful advice and expert knowledge, which significantly enhanced our understanding and approach. We are particularly thankful to Prof. S. N. Patil, Kavayitri Bahinabai Chaudhari North Maharashtra University (KBC-NMU), Jalgaon, for his support and guidance. We would also like to acknowledge the technical assistance and unwavering support provided by Dr. Ganesh Naik, Ms. Nanditha Naik, and Mr. Rakesh Nalawade during various phases of the project. Authors are also grateful to the two anonymous reviewers, for their meticulous assessment, constructive comments, and useful suggestions in improving the report.

Lastly, we would like to express our sincere gratitude to Dr. Milind Mujumdar who also happens to be a co-author on this report. His vision and initiatives were instrumental in establishing the observational site at IITM, thereby laying the foundation for this system. His extraordinary efforts, leadership, and promotion in initiating this work at IITM merit special recognition.

This work reflects the collective dedication and collaboration of all those involved, and we extend our sincere gratitude for their valuable contributions.

# Abstract

Accurate observations of field-scale soil moisture (SM) and other essential climate variables are critical for advancing weather and climate science, understanding the land-atmosphere interactions, and supporting agricultural decision-making. Conventional methods of SM measurements rely heavily on human labour that limits the scope and precision of observations. This report documents the details and performance of an Internet of Things (IoT) based hydro-meteorological monitoring system – designed to automate real-time, cost-effective observations of SM, soil temperature (ST), air temperature, humidity, pressure with phenological records. Deployed at the IITM-COSMOS site since 2019, the system comprises multi-sensor integration, wireless data transmission (Low energy Bluetooth; BLE), email, SMS, and dual power sources (solar/battery), while incorporating sensor-damage alerts for reliability. Validation against *in-situ* gravimetric measurements reveal strong agreement with sensor measurements of SM, with $R^2$ values ranging from 0.79 to 0.86 and RMSE values between 4.9% and 5.7%. Similar correspondence was noted in case of ST with an RMSE of 3.9 to 4.7 %. High-resolution data and real-time capabilities of the system addresses and improves upon the limitations of the conventional methods in field-scale data collection, offering a scalable solution for informed decision-making in climate prediction and resource management. Its modular design enables future enhancements, making it not only a versatile tool for advancing hydro-meteorological research but also suitable for agricultural applications.

# Purpose and Summary

The development of a hydro-meteorological monitoring system aims to address the critical need for accurate, field-scale observations of soil moisture and other essential climate variables that underpin advancements in weather and climate science, land-atmosphere interaction studies, and agricultural management. This report highlights the development, deployment, and performance of a field-scale, IoT-based hydro-meteorological observation system established at the IITM-COSMOS site in Pune, India. The system is designed to collect real-time, automated observations of important environmental parameters including soil moisture (SM), soil temperature (ST), air temperature, humidity, atmospheric pressure, and rainfall, along with phenological records. The goal is to overcome the limitations of conventional methods and simultaneously facilitate network approach with capacity building. The system uses a modular architecture that integrates multiple sensors built on the bed of ESP32 (python powered microcontroller) and communication technologies such as Bluetooth Low Energy (BLE), GSM/GPRS, and Wi-Fi, with dual power sources (solar and battery) for uninterrupted operation. It also includes sensor-damage alerts and augur-assisted deployment methods to ensure data quality and long-term reliability. A key contribution of this system is its ability to provide area-averaged field-scale measurements, which are more representative of actual field conditions than traditional point-based methods. It enables continuous monitoring across multiple depths and over extended time periods, capturing spatial and temporal variability in soil and atmospheric conditions. This system could prove to be an important step in terms of cost effective and reliable monitoring system for the meteorological and agricultural applications.

Overall, this report demonstrates the practical utility of developed system for real-world environmental applications. This technological advancement holds significant potential to support climate-resilient agriculture, water resource management, and broader environmental research. Additionally, the initiative contributes to capacity building by providing hands-on exposure to IoT technologies, embedded systems, and environmental data science, thereby promoting interdisciplinary skill development among stakeholders.

# 1. Introduction

Hydro-meteorological observation systems serve as essential infrastructure for multiple applications such as agricultural, meteorological, hydrological (Fangfang Huang et al., 2016). These systems integrate meteorological and hydrological measurements to provide critical insights into weather patterns, water availability, and broader climate dynamics. The data generated from these systems play a pivotal role in addressing key questions and challenges in water resource management, agricultural planning, and climate change adaptation (Stewart, 2014; Koster et al., 2004; Seneviratne et al., 2010; Whan et al., 2015; Zhang, 2004; Brocca et al., 2017). Governments, research institutions, and environmental agencies heavily rely on this data to formulate informed policies and strategies for sustainable water management (Grimes et al., 2022).

Hydro-meteorological observation systems comprise a network of strategically positioned instruments and sensors designed to collect comprehensive environmental data. These systems measure key meteorological parameters such as temperature, humidity, wind speed and direction, precipitation, and atmospheric pressure. Additionally, hydrological parameters such as soil moisture (SM), soil temperature (ST), infiltration rates, water levels, and snowpack conditions are also monitored. This systematic data collection is foundational to improving the understanding of the water cycle, weather phenomena, and environmental impacts.

The integration of cutting-edge technologies, including satellite remote sensing, automated sensor networks, and the Internet of Things (IoT), has significantly enhanced the effectiveness of hydro-meteorological observation systems. These advancements enable real-time monitoring, efficient data transmission, and improved predictive modeling, ultimately enhancing the accuracy of weather forecasts, flood predictions, and water resource management. The application of IoT has facilitated seamless data exchange across diverse hydro-meteorological applications, particularly in precision agriculture. However, challenges such as high sensor costs and the need for specialized techniques hinder the widespread adoption of these advanced monitoring systems. To overcome these barriers, cost-effective and rigorously tested solutions are required to ensure system robustness across various environmental conditions.

This report presents the development and deployment of an indigenous hydro-meteorological monitoring system as part of our training and internship program. The system incorporates soil moisture sensors, temperature sensors, and atmospheric sensors to measure variables such as temperature, humidity, pressure, and rainfall. A key feature of this system is the integration of inexpensive (low-cost) capacitive sensors for soil moisture and temperature monitoring at different depths (Deshpande et al., 2021; Chaurasiya et al., 2020, Naik et al 2023, Zarekar et al 2024). The implementation of this monitoring system follows a structured three-stage approach: (1) the initial phase involves hardware and software design, followed by (2) sensor deployment in the field at varying depths, and finally, (3) real-time data collection and analysis using diverse software tools. This report documents the system assembly, deployment techniques, calibration procedures, and the standardization of acquired data to ensure accuracy and reliability in hydro-meteorological observations. It is to be noted here, similar to any other standard SM sensors, the low-cost sensors have limitations to their accuracy and longevity. Particularly, capacitive soil moisture sensors are sensitive to environmental factors (e.g., soil texture, salinity, Sensitivity to temperature variations), and installation errors, including poor contact between the sensor. It therefore requires rigorous testing and calibration. Further improvements in cost-effectiveness and standardization are necessary to enhance the system's scalability and long-term reliability.

The report is organized as follows. Section two elaborates on the methodology and is a central focus of the objective of this report. This section includes a brief system overview, followed by details on hardware and software requirements. We then touch upon the issue of interfacing and data management. Section three deals with the particulars of on-field deployment and the related challenges regarding communication interface and data acquisition. This is followed by the section on results, comprising data analysis, calibration and validation. We then present the discussion and summary of the report and conclude with future scope.

# 2. Methodology

We begin by outlining the fundamentals of the IOT based hydro metrological system that uses a combination of low-cost (affordable), high-precision sensors to measure key atmospheric and soil parameters. It involves integration of sensing, communication, and power management, which ensures continuous, autonomous operation in diverse environmental conditions.

## a. System Overview:

A microcontroller (ESP32; Figure 1) or processor serves as a heart of this system. It is a powerful yet cost-effective embedded platform featuring built-in Wi-Fi and dual-mode Bluetooth. Its capabilities allow for real-time data processing, storage, and wireless transmission, making it suitable for applications ranging from scientific research including hydrological studies to smart agriculture and civil applications. The system combines sensors, communication protocols, and data storage for efficient hydro-meteorological applications. The system supports both wired and wireless communication protocols, enabling seamless remote access to data.

This system can incorporate a range of affordable sensors, including the atmospheric temperature, humidity and Pressure sensor (BME680), SM capacitive sensor, ST sensor (DS18B20), tipping bucket rain gauge (https://www.dfrobot.com/search-rain.html), SIM800L GSM module, SPI liquid crystal display (LCD), and ESP32 camera. The integration of these sensors play a crucial role in providing real-time analogue or digital signal values; these analogue signals are subsequently converted into digital format for further processing. These sensors are connected to General Purpose Input / Output (GPIO) pins for analogue or digital output, facilitating data acquisition and subsequent storage and transmission. The Global System for Mobile Communications (GSM) SIM module is utilized for communication, operating in various modes such as SMTP/ HTTP protocols or short message service (SMS). It is connected to the receiver (Rx) and the transmitter (Tx) pins of the controller for receiving commands and transmitting data using different protocols. The system facilitates instantaneous as well as stored output for later processing. The measured data is stored in the dedicated storage repository and transmitted at pre-defined intervals using a communication module. In addition, specific commands can be sent via SMS to the communication module using the GSM to obtain current output values from the sensors or to set new data acquisition and transmission intervals. For short-range communication, the integrated Bluetooth functionality in the main control enables communication with the mobile device or laptop.

The ESP32 CAM module connects to the microcontroller through wireless communication (WIFI). It captures the images as per the assigned time frame and stores them on the built-in SD card module on predefined time intervals. The GSM SIM800L module is controlled by the Attention (AT) commands. AT commands are also used to communicate with the sensors for retrieving current sensor outputs and sending alerts regarding sensor health and connectivity, including battery power status. The measured data from all the sensors is stored in the dedicated memory in a text format and concurrently it is transmitted using the Simple Mail Transfer Protocol (SMTP) or Hypertext transfer protocol (HTTP). All the sensors and the accessories are powered by a 2500 mAh lithium-ion battery, which has a maximum output of 12V and up to 24 hours of backup on a full charge. Interestingly the battery is rechargeable through the external power adopter or solar panel to maintain an uninterrupted power supply.

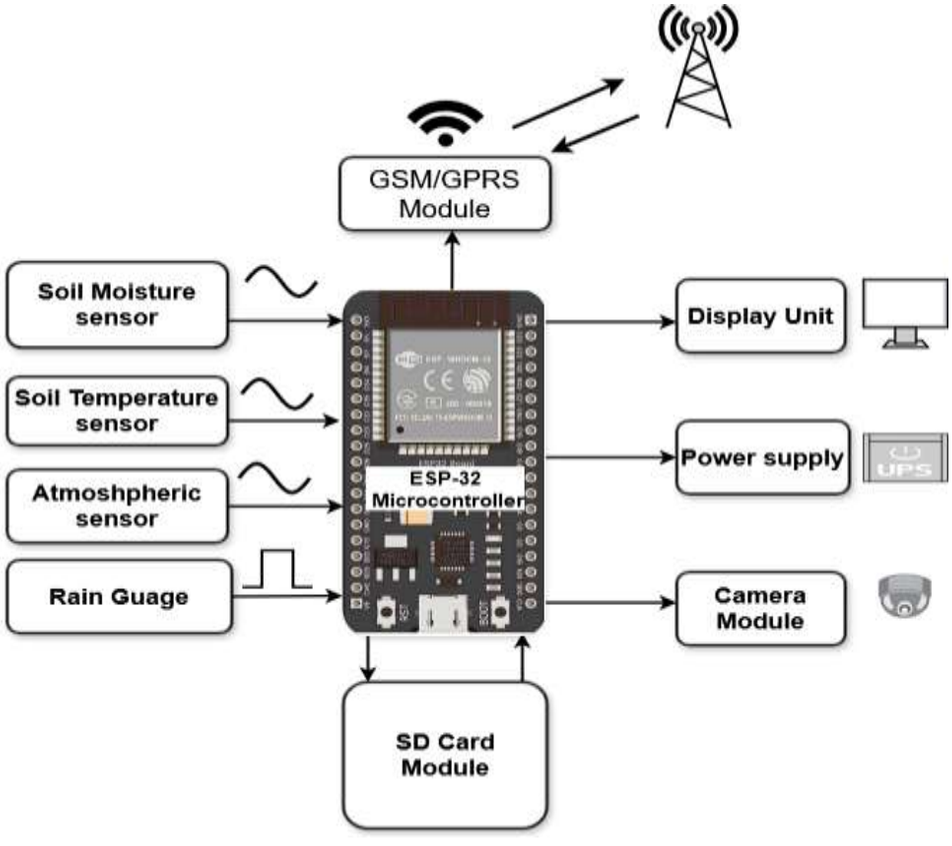


**Figure 1:** A schematic block diagram detailing the components and connections within the developed hydro-meteorological observation system.

# I. Hardware requirements

### *i. Data-Logger:*

In the field of hydro-meteorological data acquisition and monitoring, a data logger works as a central unit which records and stores critical information over time. The complex design of a data logger encompasses an array of hardware components, each playing a pivotal role in ensuring the logger's effectiveness across diverse applications. Generally, a data logger relies on connected sensors e.g., temperature and humidity sensors, pressure sensors, SM, ST, and a Rain gauge, to measure and collect data. These sensors serve as a primary measurement device, allowing the logger to capture and analyse the physical parameters based on its intended application. Basic data loggers simply collect and store data for later analysis on an external device, however advanced data loggers can process, filter and analyse the raw data in real time using built in software and algorithms. Given the requirement of the application along with cost effective design, we implemented basic data loggers. For seamless data storage, data loggers are equipped with adequate memory storage, often in the form of non-volatile memory like EEPROM (internal storage) or external options like SD cards and USB drives. This storage capacity is crucial, allowing the logger to collect a comprehensive dataset without any data loss. Sensors feed information to a microcontroller or microprocessor for data processing and transmission of data, which is the main part of the data logging system. It controls the data acquisition, storage and any additional task demanded by the application. The processing power is calibrated to the complexity of the logger's functions, ensuring efficiency and sensitivity. In the field of power supply, data loggers showcase flexibility by using either batteries or external power sources depending on the deployment requirements. Energy efficiency is a crucial consideration, particularly in situations where the longevity of the battery is a significant factor. When deploying in outdoor environments, it's important to consider the protection of the system from lightning or power leakage.

### *ii. ESP32 Microcontroller*

The usefulness of data loggers is further enhanced via communication interfaces, which make data retrieval and real-time monitoring easier. These interfaces, which create a seamless connection between the logger and external systems, could include USB, Ethernet, Wi-Fi, Bluetooth, or other wireless protocols. Along with incorporating displays and operational controls, a user-friendly interface is another common component of a data logger. Through performing this, users may improve accessibility and usability by directly retrieving information from the logger, monitoring statistics, and configuring settings. The logger is protected from weather conditions by a robust enclosure that is capable of handling moisture, dust, and extremely high or low temperatures. Data loggers employ real-

-time clocks or synchronize with external time sources to maintain temporal precision, ensuring accurate precise time stamping of recorded data. Moreover, precision in soldering and attention to power efficiency is paramount to maximize the logger's operational lifespan. The approximate cost of the entire hydro-meteorological system is about ₹ 30-35 thousand. Overall, well-designed and assembled logger circuit hardware is fundamental for creating a robust data logging device tailored to specific environmental or research ESP32 is the main controlling unit for this comprehensive standalone system (see Figure 2). This microcontroller utilizes 40 (nm) nanotechnologies, which provides robustness and extensive integration. This control unit is a compact single chip device, which incorporates many features, such as Bluetooth, Wi-Fi, a coprocessor with extremely low power consumption, and multiple peripherals. The ESP32 chip acts as the module's central processing unit, offering a flexible and adaptive design. Its central processing unit (CPU) clock frequency can be adjusted in a range from 80 MHz to 240 MHz, and it boasts two independent CPU cores. Additionally, the chip incorporates a low-power coprocessor, which proves invaluable for energy-efficient execution of tasks that require minimal processing power, such as peripheral monitoring. The ESP32 is equipped with a wide array of integrated peripherals, including capacitive touch sensors, an SD card interface, Ethernet, high-speed SPI, UART, I2S, and I2C. Notably, the ESP32 chip consumes about 240 mA of power, which makes it ideal for battery-operated and portable devices. With integrated Bluetooth, BLE, and Wi-Fi, this module is versatile and suited to a wide range of applications. Wi-Fi connectivity ensures an extensive physical range and direct internet access via a Wi-Fi router. Bluetooth functionality provides convenient smartphone pairing and the ability to broadcast low-energy beacons for detection. Consequently, the module excels in electronic integration, range, power efficiency, and connectivity, setting industry standards in these parameters. The system is programmed using Micro Python, effectively controlling all aspects of its operation.

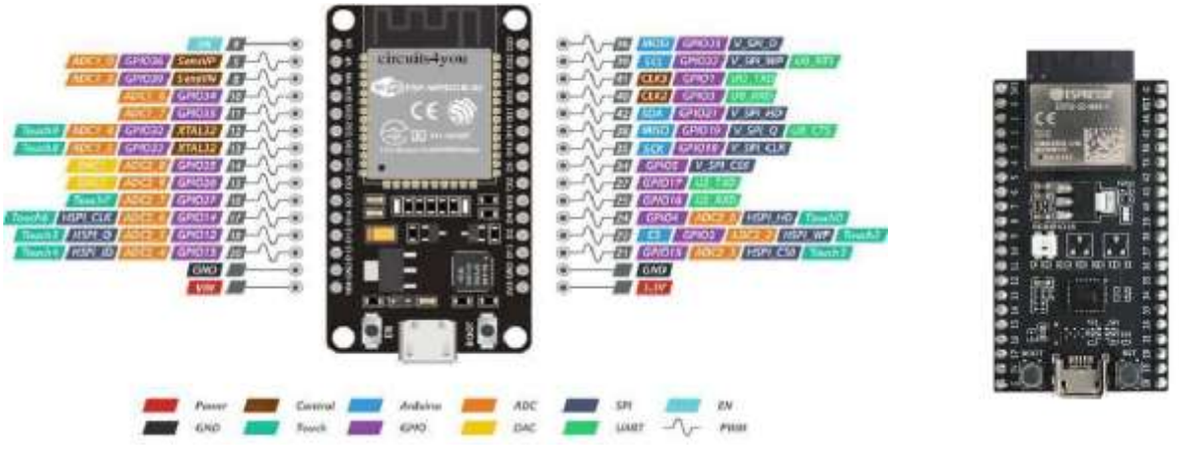


**Figure 2:** Pin configuration of the ESP32 microcontroller module, providing a visual representation of the arrangement and classification of its pins.

### *iii. GSM/GPRS SIM 800l:*

An efficient communication between any logging device and end user such as mobile, computer or any server requires a dedicated device. To establish this communication a specialized compact circuit is


**Figure 3:** Pin configuration of GSM SIM module

developed, commonly referred to as a GSM module or GPRS module. This device facilitates seamless data communication through mobile towers. This module is equipped with a modem (modulator-demodulator), which is essential for the pre- and post- processing of the transmitted data. Activation of the communication with the network is contingent upon the insertion of a SIM (Subscriber Identity Module) card, much like in mobile phones. Additionally, these modules possess IMEI (International Mobile Equipment Identity) numbers, akin to mobile phones, for identification purposes. This study incorporates the SIM800L module for GSM/GPRS applications. The SIM800L modem operates in response to AT commands. These AT commands serve as the means of interaction and control between the ESP32 module and the SIM800L modules. The ESP32 module dispatches AT commands to the SIM800L module to regulate various functions, including SMS and EMAIL operations, among others. This module utilizes the date and time information of the network provider for the data recording and communication purpose.

### *iv. Capacitive Soil Moisture Sensor:*

Various types of sensors are used for soil moisture (SM) measurement, including resistive, electromagnetic, inductive, capacitive, and neutron monitoring sensors. In the present study, a capacitive soil moisture sensor is deployed in the field due to its low cost, efficiency, and suitability for continuous monitoring. A capacitive soil moisture sensor estimates the water content of the soil by detecting variations in its dielectric properties. This principle is based on the fact that water has a significantly higher dielectric constant (~80) compared to dry soil (ranging from 3 to 7) and air (around 1) (Abdelmoneim et al., 2025). These differences allow the sensor to infer soil moisture levels by sensing changes in the dielectric constant of the medium surrounding it. Typically, a capacitive

sensor consists of two metal plates or conductive surfaces that form a capacitor. These plates are placed inside or close to the soil. When an electric field is applied across the plates, the sensor behaves like a small capacitor, with the soil acting as the dielectric material. As the moisture content in the soil changes, the dielectric constant changes accordingly, thus altering the capacitance, which the sensor detects. In this setup, a 555-timer integrated circuit is used to convert the resonance frequency of the sensor into an analog voltage signal. This analog signal can be directly read by a microcontroller unit such as the ESP32, which further converts it into a percentage-based soil moisture reading (Lyons, R. G., 2011). The sensor operates within a voltage range of 3.3V to 5.5V, making it compatible with a variety of low-power microcontrollers.

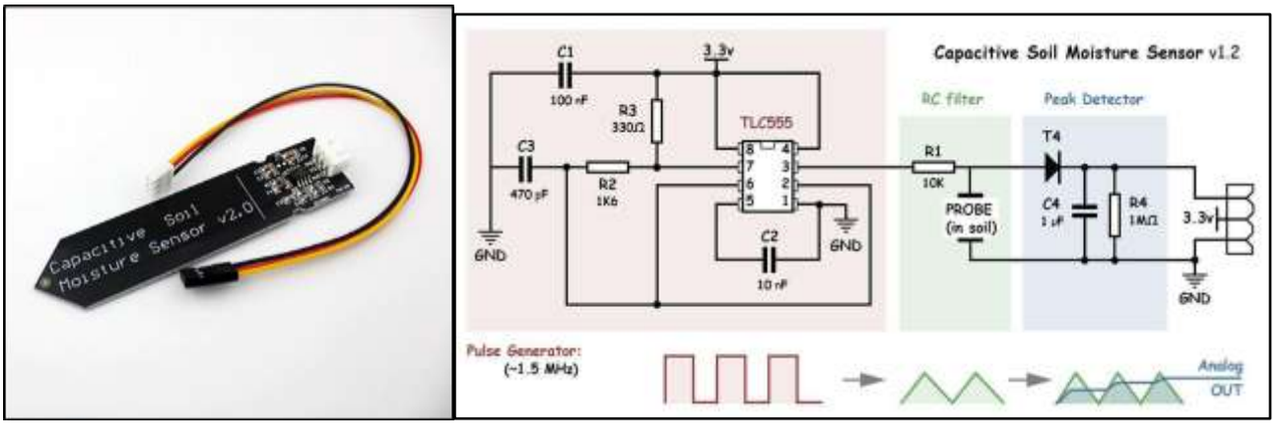


**Figure 4:** Capacitive-type soil moisture sensor (left panel) and its circuit diagram (right panel).

$$\text{Digital Value} = \frac{\text{Analog Voltage} - V_{\min}}{V_{\max} - V_{\min}} \times (2^N - 1) \quad (1)$$

where: Analog Voltage is the input voltage you want to convert. $V_{\min}$ is the minimum input voltage that corresponds to a digital value of 0. $V_{\max}$ is the maximum input voltage that corresponds to a digital value of $2^N - 1$. (Which is the highest possible digital value in an N-bit (ADC, 8 in this case) digital system. The moisture availability in the soil affects the capacitance of the circuit, consequently affecting both the peak amplitude of the signal and the measured DC voltage output by the main controlling unit (MCU). Higher moisture levels result in lower DC voltage output. The capacitive sensor doesn't use the electrical current during the measurement of SM, which reduces the risk of electrolysis. However, this probe has its weaknesses, primarily related to its exposed electronics at the top and the uncoated cut edges of the PCB. Over time, these exposed areas can collect moisture, potentially shortening the probe's lifespan. To avoid this shortening, we covered the exposed part of the sensor using the epoxy resin coating, which is a good insulator in protecting the sensor from moisture or rusting. The necessary wiring connections are described in the further subsection. All measurements displayed after the required calibration and validation.

### *v. DS18B20 Temperature Sensor:*

The DS18B20 Digital Thermometer offers 9 to 12-bit temperature measurements that are configurable to display the device's temperature. It requires only one wire and a ground connection from a MCU to the DS18B20 since digital data is transmitted to and from the DS18B20 using a 1-Wire interface. For operations like reading, writing, and performing temperature conversions, it can take power directly from the data line, doing away with the requirement for an additional power supply. Multiple DS18B20 sensors can be operated using 1-Wire bus, because every DS18B20 has a unique silicon serial number. This feature enables the use of temperature sensors in various locations, making it applicable to scenarios such as process monitoring and control, environmental regulation in Heat, Ventilation, and air conditioning (HVAC) systems, temperature measurement within buildings, machinery, and equipment (Saha et al., 2020.).

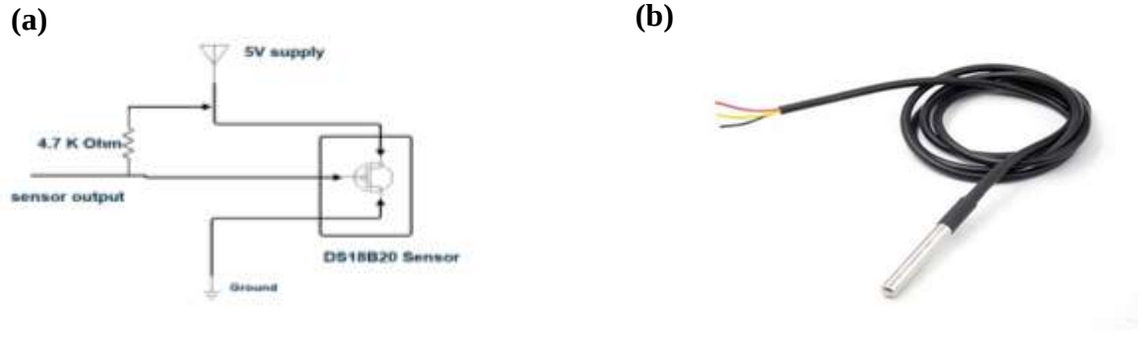


**Figure 5: (a)** The circuit diagram and **(b)** Representation of DS18B20 temperature sensor.

### *vi. BME680 Environmental Sensor:*

The '*7Semi BME680*' Sensor Probe is a cost-effective solution designed for monitoring atmospheric variables. This sensor probe consists of an Inter-Integrated Circuit (I2C) interface to seamlessly communicate real-time data of temperature, humidity, pressure, and gas levels. The BME680 sensor is enclosed in a robust plastic casing for a longer service life, ensuring a safe and comfortable atmosphere. For the outdoor applications this sensor is covered with a protective shield (see Figure 6b). The sensor requires very less power (1.7 to 3.6 V) for the operation. Sensor communicates with the main controlling unit (MCU) through the connecting cable. The 7Semi BME680 Sensor Probe is a cost-effective solution designed for monitoring atmospheric variables. This sensor probe consists of an Inter-Integrated Circuit (I2C) interface to seamlessly communicate real-time data of temperature, humidity, pressure, and gas levels. The BME680 sensor is enclosed in a robust plastic casing for a longer service life, ensuring a safe and comfortable atmosphere. The BME680 is developed by Bosch Sensortec (https://www.bosch-sensortec.com/products/environmental-sensors/gas-sensors/bme680/)

for various applications, including healthcare, HVAC, agriculture, and soil monitoring. A cutting-edge environmental sensor capable of measuring temperature, humidity, barometric pressure, and gas levels. This 4-in-1 digital sensor provides accurate and dependable data in various atmospheric conditions. Notably, the BME680 features a highly sensitive and accurate sensor, making it an ideal solution for environmental monitoring applications.

**(a)** **(b)**

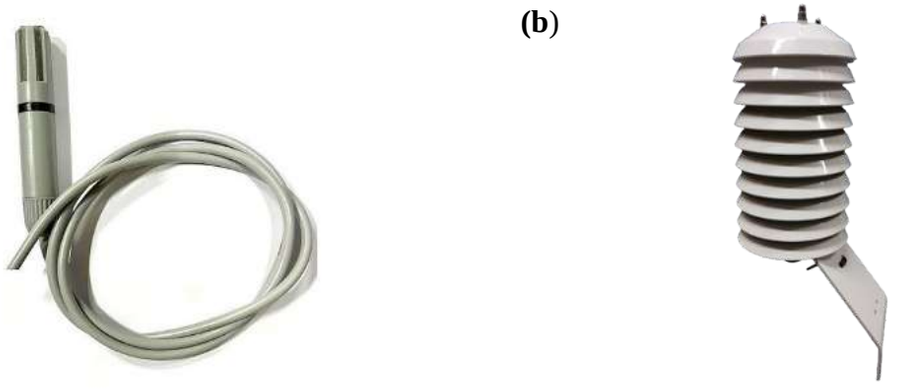

**Figure 6: (a)** All in one sensor system which measures temperature, humidity, and pressure in the atmosphere and **(b)** Protective shield of the sensor.

### *vii. Tipping Bucket Rain gauge:*

The measurement of rainfall using ground-based sensors is crucial for hydrological research, basin water balance assessments, storm frequency analysis, hydraulic infrastructure design, meteorological radar calibration, and flood forecasting (Bournas & Baltas, 2023). Among the various types of automatic rain gauges, the tipping bucket rain gauge (TBR) is one of the most widely used for measuring real time rainfall intensity. As described by Segovia-Cardozo et al. (2023) and Krüger et al., (2024), TBRs are preferred due to their simple design, low manufacturing cost, and energy efficiency, making them a preferred choice for national meteorological services, industries, and private applications. These gauges serve as the primary data source for calibrating radar-based rainfall estimates, ensuring more accurate hydrological forecasting and analysis (Ochoa-Rodriguez et al., 2019). Interestingly, due to the particulars of design which consists of hollow bottom, facilitating automatic drainage eliminates the need for electronic components inside. This device can be easily integrated into multiple platforms and is compatible with micro: bit, ESP32, Arduino and Raspberry Pi. It also supports I2C and UART (Universal Asynchronous Receiver/Transmitter) data output protocols. Prebuilt Go libraries simplify the setup of rain monitoring systems, while the Gravity interface enhances the user experience. This versatile device finds applications in weather monitoring,

environmental tracking, smart farming, research, and education. The specifications include a working voltage of 3.3 to 5.5V DC, a low working current of less than 3mA, and I2C/UART output digital signals. With a high resolution of 0.28 mm per tip, it operates over a wide temperature range from -40° to 85°C. The mounting hole size of 3.1mm further facilitates easy installation, making this rain monitoring system an invaluable tool for comprehensive environmental data collection.

**Figure 7:** The experimental tipping bucket rain gauge installed at KBC-NMU, Jalgaon.

***viii. ESP32 Cam module:***

Vegetation and atmospheric conditions play a major role in the land atmosphere energy exchange. It is therefore necessary to monitor vegetation and atmospheric conditions using the phenology camera, which can be achieved by the ESP32 cam module incorporated in this system. This ESP-32 cam module consists of a 2MP camera with inbuilt Wi-Fi and Bluetooth. This module is comparatively small and can operate independently as a compact system with a footprint of only 40 x 27 mm. Given its less power consumption (6mA), this module is widely used in various IoT applications such as field scale monitoring of vegetation, home smart devices, industrial wireless control and wireless monitoring. This module has a DIP packaging and can be installed straight into the backplane to support fast product manufacturing. It features a high-reliability connection mode, making it suitable for use in a range of IoT hardware terminal applications. ESP32 cam combines two very efficient 32-bit CPUs with Wi-Fi and conventional Bluetooth. The primary frequency adjustment range of this device is 80MHz to 240MHz. This device can be synchronised with the MCU of the main ESP-32 module for further processing of the collected images which are then stored in a dedicated memory slot.

**(a)** **(b)**

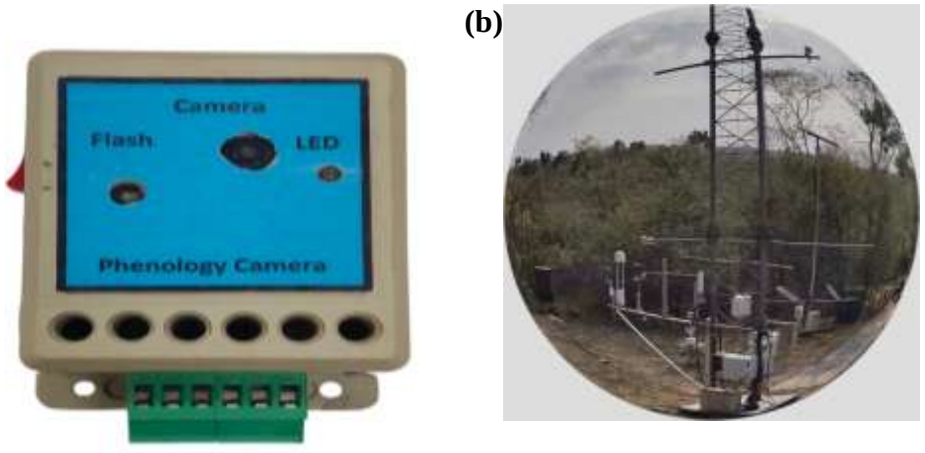


**Figure 8: (a)** ESP-32 Cam module for Phenology camera and **(b)** an image taken by the Phenocam.

### *ix. Power Unit:*

Any instrument or circuit should have a designated, continuous power source to meet its power requirements. In this study, we integrated a power source which is a combination of a number of power sources, such as a solar unit, regulated power source, and a battery bank to efficiently manage the required power demand. This integrated power unit is lighter and more compact than the other Power units such as Ni-Cd, Ni-MH, and Lead Acid Batteries.

The internal charge protection circuit within the battery pack allows for direct charging using a DC power adapter, eliminating the need for specialized battery chargers and concerns about overcharging. This multipurpose power source, with its high energy density, resistance, and voltage, produces consistent performance over time. High capacity, a low discharge rate, ability to reach full charge within 40-90 minutes and maintaining a reliable output voltage of 12V makes it a suitable power source for the intended application. This system measures the data at every 15-minute interval, which facilitates an optimal balance between temporal resolution and power efficiency. Depending on environmental conditions and communication type, current configuration allows for 5-6 days of operation on battery power on single charge. In the broader context of this project, we seamlessly integrated the LM2596 series of monolithic integrated circuits to address the power regulation. These circuits, having load regulation, up to 3.0A are designed for efficient implementation. When working with higher input voltages switch-mode power supplies such as the LM2596 converter offer significantly more efficiency than conventional three-terminal linear regulators. Key features of the LM2596 include a guaranteed +/- 4% output voltage tolerance under specified input voltages and load conditions, coupled with a +/-15% variation in the oscillator frequency (+/- 2% over the temperature

range of 0°C to 125°C). The LM2596 used here can handle input voltages between 4.5 and 40V and producing output voltages between 3 and 35V.

**(a)** **(b)**

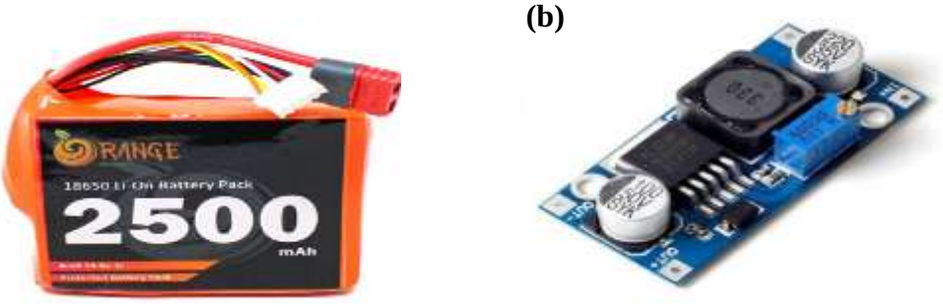


**Figure 9:** Power unit consisting of: **(a)** Lithium battery and **(b)** the DC buck converter to provide continuous and regulated power to the entire system.

The potentiometer on the buck converter enables easy adjustment of the output voltage as required. This integration provides an accurate and flexible solution for all kinds of power demands in this instrument or circuit, in addition to increasing the overall efficiency of this power system.

### *x. SD card Module:*

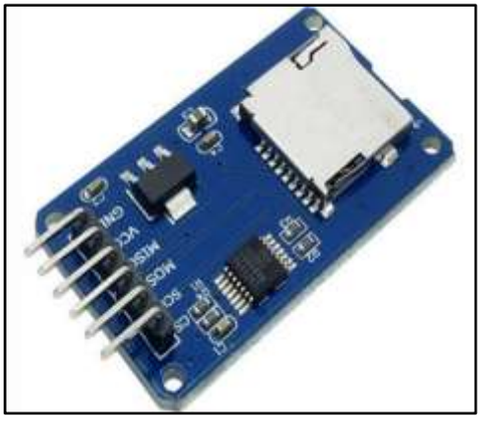

**Figure 10:** SD card module for data storage.

Data acquisition is the main component of any data monitoring device. The internal memory of the ESP-32 is not sufficient for storing the measured data and program files. This study uses a dual input output (I/O) supported Micro SD card (dedicated memory) module, known as Miro SD Adapter. The module provides a feature of easy reading and writing data. Also, this module seamlessly configures various microprocessor or microcontroller devices. This device operates on a voltage range of 3.3-5V, which is compatible with the ESP32 and Adriano and features a serial peripheral interface (SPI) that works with any SD card. This module is used in various applications such as data logger, audio, video, and graphics.

### *xi. Thin-film-transistor Liquid Crystal Display (TFT-LCD)*


**Figure 11:** Liquid Crystal Display for visualizes of the measured data.

The implementation of an LCD display into a logging device is essential for improving its accessibility and identifying malfunction at an early stage. During logging operation, the display functions as a primary interface, providing real-time visualization of data. Operators can efficiently monitor various parameters, enabling quick checks of status that can lead to an accurate decision-making. The operator can submit commands, modify settings, and receive instant feedback. This study uses an LCD display with a resolution of 128 x 160 pixels and can show 18-bit colours. It operates on a voltage range of 3.3-5 Volt.

## II. Integrated Hardware Assembly and Circuit Design of the hydro-meteorological system:

An essential stage in the development of any electronic devices is hardware assembly, which acts as a link between conceptual design and final developed product. In order to ensure proper connectivity with respect to the design criteria, and practical implementation, this process requires a careful integration of distinct electronic components into an integrated unit. It includes important aspects like quality control, manufacturing, and scalability. For monitoring and acquiring field-scale hydro-meteorological data, a specialized circuit has been designed (see Figure 12). In this system controller plays a major role in controlling all the connected devices and sensors. Also it provides necessary power to the components. All the necessary pin configurations and wiring details of all the sensors are shown in Table no. 1. The general purpose input output (GPIO) pins are used to communicate analogue (capacitive SM) and digital (ST, rain gauge and atmospheric temperature, humidity and pressure) sensors to microcontrollers. Additionally, the SDA and SCK GPIO pins are used for the I2C communication protocol. The communication module called GSM/GPRS SIM 800L is connected to the receiver (Rx) and transmitter (Tx) pins and DC to DC buck converter which is indirectly connected to the ESP32 for controlling the power supply. Moreover the ESP32 cam module is connected to the main controller through the wireless media (WI-FI). The programming language used in this study is the Micro python.

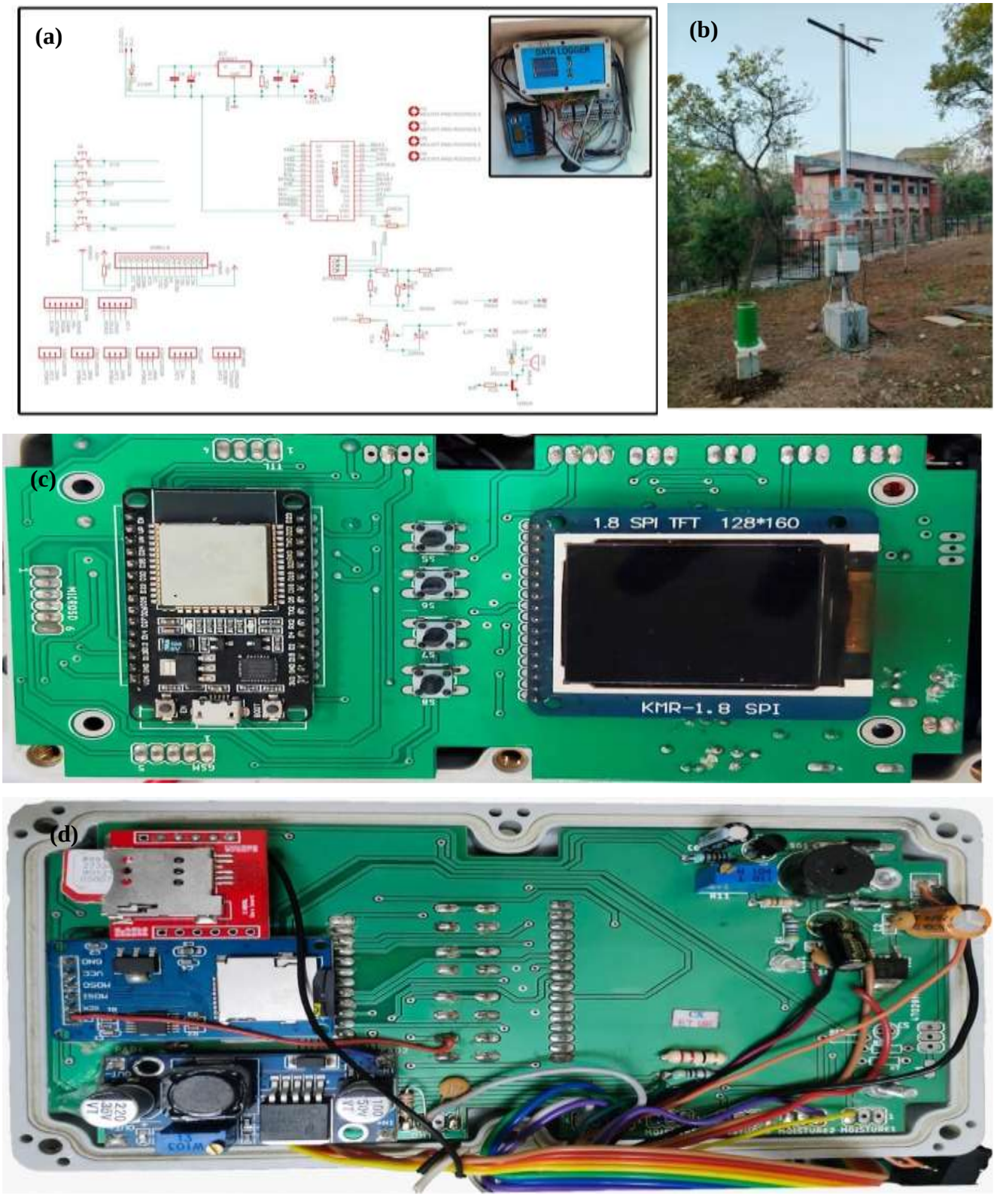


**Figure 12: (a)** Schematic circuit diagram of the Hydro-meteorological observation system, with inset depicting the final product. **(b)** The complete set up. Panels **(c)** and **(d)** shows top and bottom sides of the actual integrated dual sided printed circuit board (PCB) with electronic connections and components.

**Table 1:** Wiring details for all sensors and supporting modules within the logging system.

| Sr. No | Sensor Description | Wiring Details | ESP-32 pin |
|---|---|---|---|
| **1** | Soil moisture sensor 1 | Red (Positive supply) | D32 |
| | | Blue (Data) | |
| | | Black (Negative supply) | |
| **2** | Soil moisture sensor 2 | Red (Positive supply) | D34 |
| | | Blue (Data) | |
| | | Black (Negative supply) | |
| **3** | Soil moisture sensor 3 | Red (Positive supply) | D35 |
| | | Blue (Data) | |
| | | Black (Negative supply) | |
| **4** | Soil moisture sensor 4 | Red (Positive supply) | D36 |
| | | Blue (Data) | |
| | | Black (Negative supply) | |
| **5** | Temperature sensor (DS18B20) | Red (Positive supply) | D2 |
| | | Black (Negative supply) | |
| | | yellow (Data) | |
| **6** | BME-680 | Red (Positive supply) | |
| | | Black (Negative supply) | |
| | | White (SCL) | GPIO21 |
| | | Brown ( SDA) | GPIO22 |
| **7** | Rain Gauge | Red (Positive supply) | D1 |
| | | Black (Negative supply) | |
| **8** | Sim 800l | NET | NA |
| | | VCC(connect via buck converter) | 5V |
| | | RST | NA |

| | | | |
|---|---|---|---|
| | | RXD | TX |
| | | TXD | RX |
| | | GND | GND |
| **9** | Liquid Crystal Display (LCD) | MISO | NA |
| | | CS | GPIO 15 |
| | | SCL | GPIO 18 |
| | | SDA | GPIO 23 |
| | | DC/SPI | GPIO 2 |
| | | Reset (Rst) | GPIO 5 |

### *i. Main Functioning script:*

Upon powering on, the main functioning script initiates the system by coordinating several essential procedures. It begins by initiating the Sim800L (GSM/GPRS) and setting up a Wi-Fi server to establish connections with the camera, Bluetooth, and other devices. The script then configures parameters for all connected devices and acquires the date and time for the ESP32 RTC from the Sim800L GPS. Then, it displays with various sensor values, including ST, moisture content, air humidity, and temperature. As part of its functionality, the script monitors the stored time, facilitating the periodic (daily) storage of data in the DATA.txt file and instructs the Digital Camera to capture and store an image in the camera's SD memory on hourly scale. Additionally, the system is designed to dispatch SMS notifications in case of sensor faults and low battery voltage. An automated EMAIL transmission of the text file is triggered at predetermined intervals. The script continuously monitors SMS and Bluetooth commands, including READ, STORE, and SET_STORE, ensuring interactive control and seamless communication with the system. This comprehensive sequence of operations ensures efficient data management and real-time monitoring capabilities.

### *ii. Data acquisition module:*

Data acquisition is an important component of this system, which is capable of collecting data at the maximum frequency of 1Hz. However, given the persistence exhibited by different hydrometeorological variables we opt for the period of 15 minutes between consecutive data collection (recording) for all sensors. These sensors include SM, ST, pressure, and humidity sensors. The script contains functions beyond simple data acquisition, incorporating calibration functionality to ensure accurate readings in technical terms. These functions not only provide the acquired data from the sensors but also offer insights into any identified faults within the sensor system. This approach enhances the script's value by not only making data collection easier but also allowing for detection and reporting of potential errors, which improves the entire system's durability and consistency.

### *iii. Bluetooth module:*

A python script for the Bluetooth module configures ESP32 as a Bluetooth Low Energy (BLE) Server, which enables seamless interaction with other Bluetooth clients. By initializing the ESP32, the script enables external devices to connect and communicate with the system. The script includes functions that are specifically designed to establish and maintain Bluetooth communication. These functions provide a basis for managing the complexities of communication protocols, ensuring a reliable and strong connection between the ESP32 and Bluetooth clients. Therefore, it enhances the scope of interactions and system's adaptability by allowing other devices to communicate via Bluetooth.

### *iv. Date time module:*

Storing the data with a time stamp and regulating periodic activities (e.g., relaying scheduled email) are essential and are carried out by the date time script. The function that checks store time determines if the current time matches to the scheduled time for storing data in SD memory and capturing images and accordingly executes these tasks. Similarly, the *Auto_Email* function is designed to check whether the present time meets the criteria for triggering the auto email feature. In summary this script contributes to the automation capabilities of the system by adding appropriate time stamps.

### *v. SD card module*

The script that interacts with the SD card serves as a specialized function dedicated to storing and managing data files on a SD card within the system. It incorporates essential functions customized for storing data files in text format. This script works with the date-time script described above and both the *main* and other programs call upon this script for writing and reading the data. The stored data formatted as a text file is transmitted using email (e.g., invoking an *auto_email* function) over RS232. The modular design improves code readability and sustainability that streamlines data processing.

## V. Software requirement:

The software requirements for any logger circuit are as crucial as its hardware requirements. It plays a vital role in data acquisition, processing, and storage. A microcontroller or microprocessor is typically programmed into a firmware or an embedded software to manage the operation of the logger. It is important that the software has been designed so that it facilitates smooth and seamless interaction between the hardware components, sensors, data flow control, and storage system management. It includes algorithms for data processing, error handling, and ensuring the accurate time stamping of recorded information and battery status (figure 13). The software design must also consider user interfaces for configuration, data retrieval, and possible wireless connection. The programming should prioritize efficiency and optimization to extend the logger's battery life in cases where power conservation is critical. Regular updates or calibration procedures may also be part of the software requirements to maintain accuracy over time. In summary, the software for a logger circuit is essential for the proper functioning of the device, enabling it to fulfil its data logging tasks accurately and reliably.

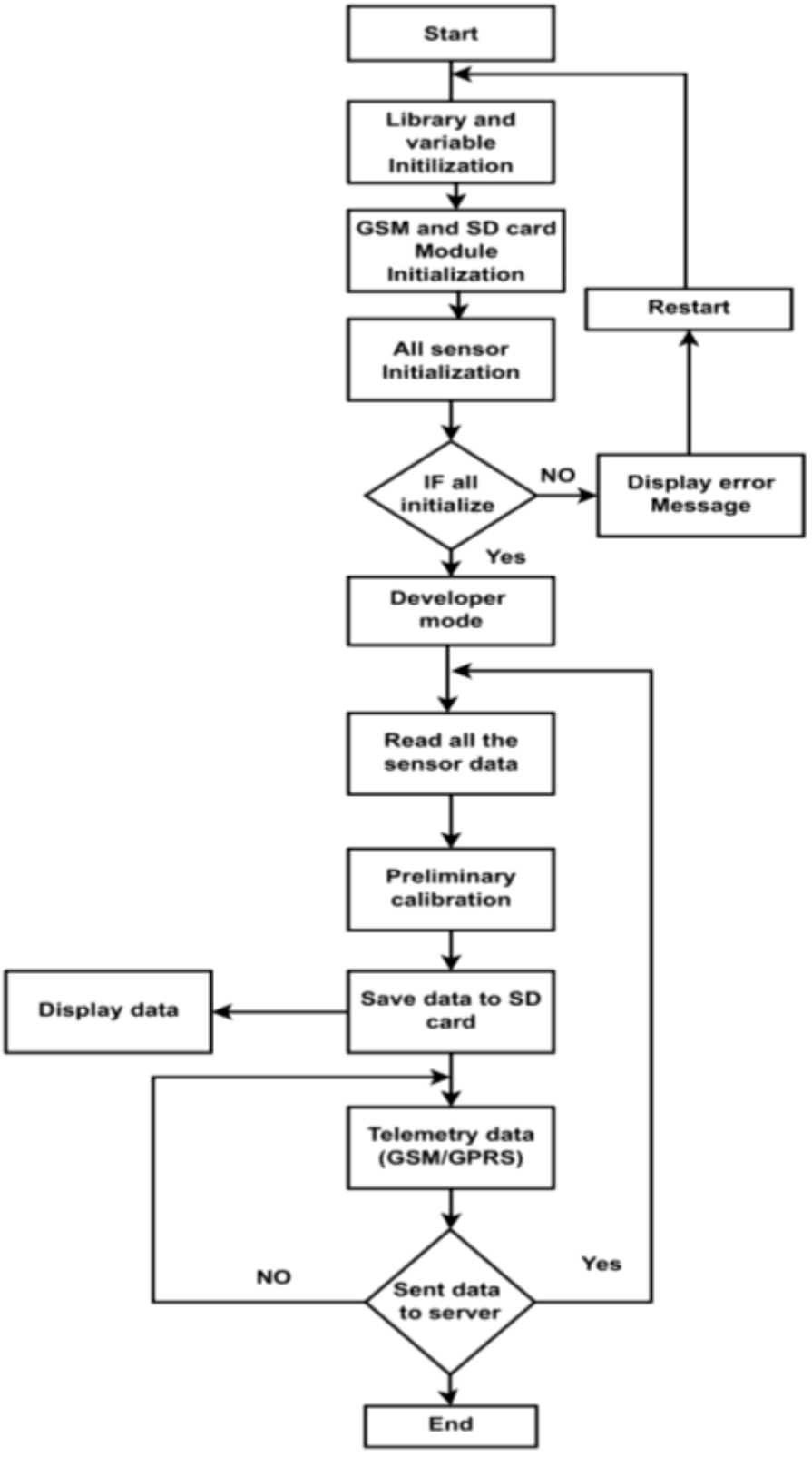


**Figure 13:** Sequential steps (algorithm) indicating the sensor initialization, data archiving, and transmission process.

## b. Field deployment of sensors at various depths

This research project focuses on the in-house assembly of a hydro-meteorological system, with the potential to expand into a field-scale observation network (200–300 m) at the IITM-COSMOS Pune site (Fig. 14**a**). The site is located on the campus of the Indian Institute of Tropical Meteorology (IITM), Pune, at approximately 18.5374°N latitude, 73.8054°E longitude, and ~560 m above mean sea level. The site is a part of the Deccan Plateau, within the meteorological subdivision of Madhya Maharashtra (Guhathakurta et al., 2015). Importantly, it lies within the core monsoon zone of India (Rajeevan et al., 2010), a region characterized by strong land–atmosphere coupling (Ganeshi et al., 2020). The site receives southwest monsoon rainfall during June to September (average accumulated monsoon rainfall is about 680 mm, (Guhathakurta et al., 2015; Revadekar et al., 2015) and is recognized as an area of strong soil moisture–temperature coupling (Ganeshi et al., 2020). More than 75% of the site largely consists of natural forest with average tree heights (8-10 meters) being constant around the year. Additionally, during monsoon bushes, grasses and forbs are also observed. The chemical and physical analysis of the soil indicated significant heterogeneity (both vertical and horizontal, in terms of soil type and texture) with a mild gradient from the southeast to the north. The site has been operational since January 2017.

To obtain field-scale SM estimates a strategy proposed by Franz et al., (2012) was adopted and optimized for the site. We constructed three concentric circles of radii of 5 m, 25 m, and 75 m with COSMOS probe tower as a centre (Fig. 14**b**). The 5 m inner circle captures local variability near the probe, important for assessing short-range heterogeneity, root distribution, and management effects. The intermediate circle (25 m) represents midrange variability within the footprint, while the outer circle (75 m) characterizes far-field conditions within the COSMOS sensing radius. Together, this radial distribution captures gradients in soil properties and moisture content across the footprint. Sensors were deployed at multiple depths along these circles (indicated by red dots).

To further strengthen spatial representation, the site was divided into four quadrants—North, South, East, and West. Within each quadrant, one profile was established to account for directional influences such as slope orientation, shading, prevailing winds, or vegetation distribution. This combined radial–quadrantal design produced nine sensor profiles in total, each with four measurement depths, enabling a detailed characterization of SM dynamics across the footprint. Calibration and validation were carried out by collecting soil samples for gravimetric analysis from the surface to 1 m depth at 10 cm intervals, across multiple locations within the site (indicated by brown dots). For calibration and validation of assembled and standard sensors, the gravimetric

measurements are converted to volumetric SM (in %, Equations 2 and 3 in Section 3a). These samples provide a robust benchmark for evaluating the performance of in-situ sensors and correcting for site-specific effects (see Section 3b for details).

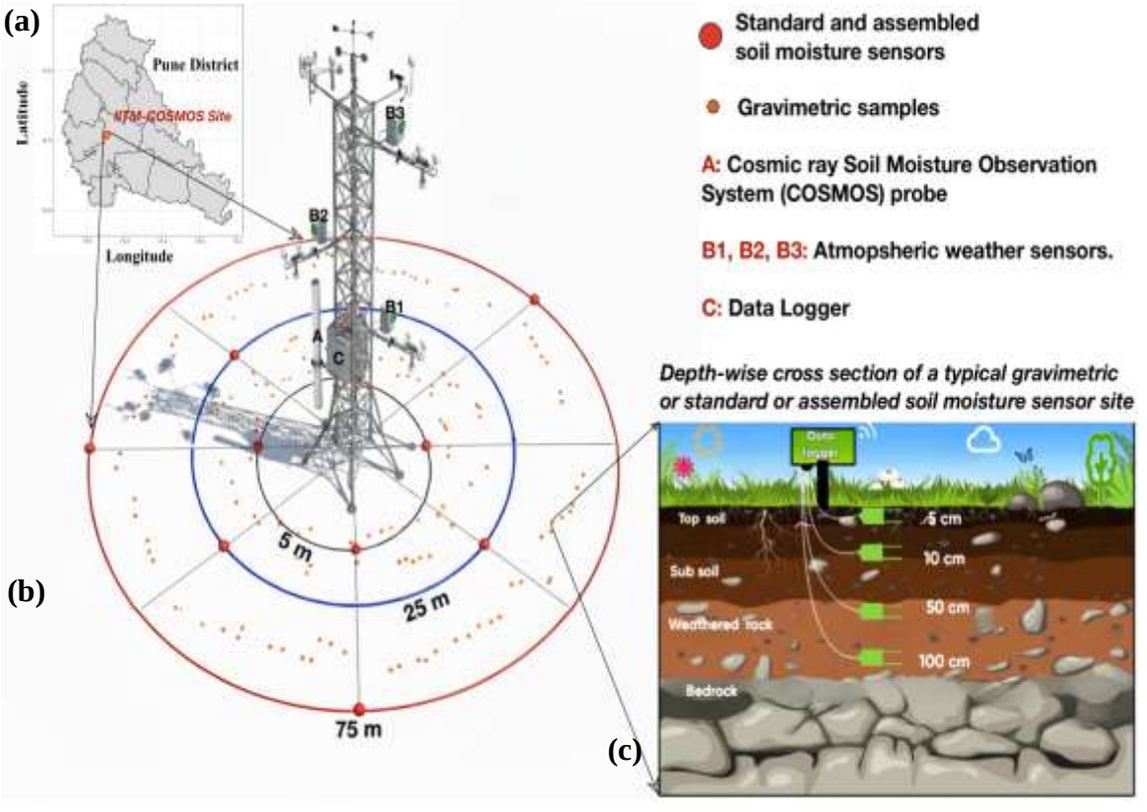


**Figure 14: (a)** Map of the Pune district showing the location of IITM-COSMOS site (Orange circle). **(b)** Visual representation of the observation network, highlighting different measurement sensors: including IITM-COSMOS tower, standard and assembled sensors (red) and locations of gravimetric observations (brown dots), **(c)** Schematic of sensor deployment at various depths, providing a comprehensive overview of a vertical distribution and arrangement of sensors.

Deploying SM sensors at various depths across the field-scale is crucial for comprehensively understanding soil hydrology and soil water dynamics (Goswami et al., 2023; Ingale et al., 2025). Many research studies have chosen specific depths based on their study objectives, such as surface soil (0–15 cm), root zone (15–30 cm), and sub-surface (30 cm and beyond) (Fan et al., 2024; Jobbágy and Jackson, 2000; Goswami et al., 2023). This study incorporates sensors at four different depths namely 10 cm, 30 cm, 50 cm, and 100 cm (Figure 15). The installation process involves carefully placing sensors using tools like soil auger (Figure 15 **c** and **d**) while maintaining the soil texture. Proper calibration, with adequate sensor spacing and regular maintenance are crucial for accurate and reliable data collection.

Assimilation of data from various soil depths is essential to understand soil water dynamics which in turn can improve numerical weather prediction (NWP) and the forecasting skills. Advanced assimilation approaches combine observations of SM and ST from multiple depths, to provide an accurate description of the current soil condition. This information is crucial for initializing NWP models. The accuracy of these initial conditions can improve the representation of the exchange of heat and moisture between the land and the atmosphere. Beyond meteorological applications, this information is also helpful for understanding the soil hydrology as well as the precision agricultural applications enabling farmers to adapt irrigation practices specific to soil conditions. Moreover, the integration of multi-depth data supports in-depth research on root development, soil structure, and surface-subsurface water dynamics, providing a holistic understanding of soil profiles and contributing to sustainable land management practices.

Practically, the deployment of soil sensors in agricultural settings offers a dynamic framework for real-time monitoring and data acquisition. These sensors, designed to measure key soil parameters such as moisture content and temperature, facilitate a nuanced understanding of the soil environment. The wireless connectivity options associated with these sensors further increase their usefulness by enabling continuous data transmission, thereby providing researchers and stakeholders with timely and remote access to critical information. As technology advances, integrating sensor data with other environmental parameters becomes increasingly important for creating resilient and sustainable farming practices. Overall, deploying soil sensors at different depths is a key strategy for understanding the surface-subsurface processes, land-atmosphere energy exchanges, modelling activities and precisely managing agriculture practices for a sustainable approach to land management.

Deploying a profile sensor at field-scale is often a labour-intensive and time-consuming process. To obtain precise and accurate data, the position of the sensor during the deployment should be kept horizontal. Traditional methods of digging earth pits for sensor placement can disrupt soil texture and contribute to prolonged settlement times. In view of the requirement for a more efficient and less intrusive approach, an augur was developed with the help of mechanical engineering students under the IITM internship program. Utilizing a simple yet effective screw gauge mechanism, the augur, a unique innovation, has significantly streamlined the sensor deployment process. With clockwise rotation augur descent into the soil, allowing for the collection of a soil core measuring 20 cm x 20 cm (width × depth). In 5 attempts (digging upto 20 cm in each attempt), the augur can reach up to 1 meter in soil. This unique approach not only expedites the deployment process but also minimizes soil disturbance. After collecting the soil core, the sensor is carefully inserted, and the core

is returned to its original position using the augur, ensuring minimal disruption to the surrounding environment.

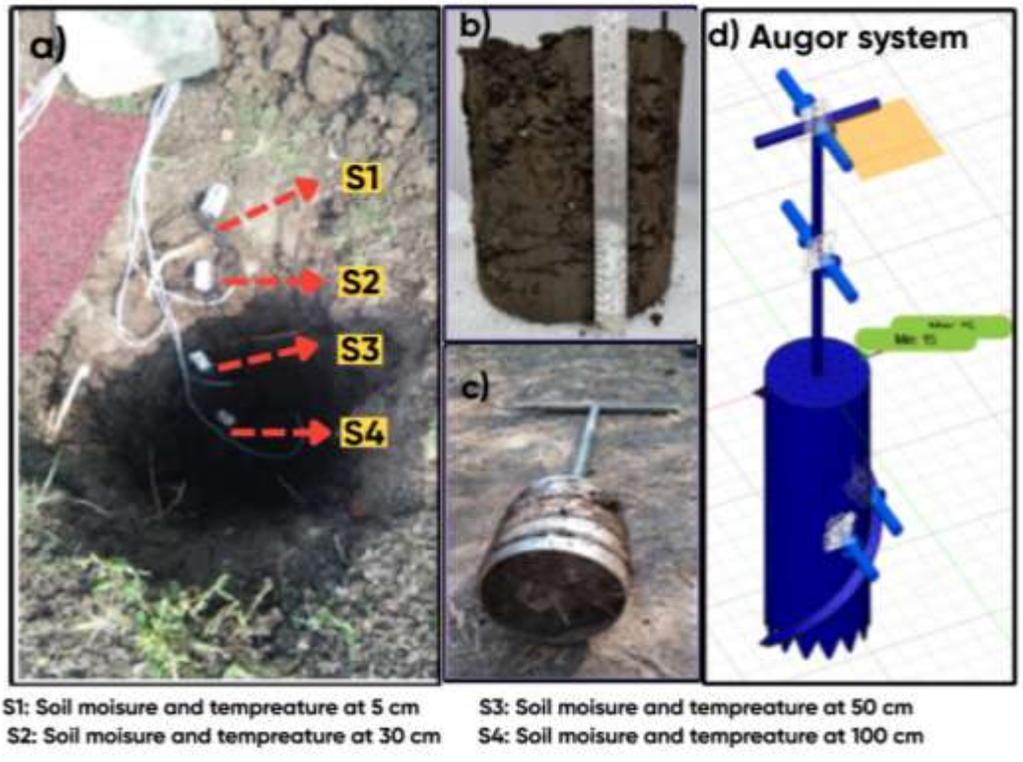


**Figure 15: (a)** Deployment of soil sensors at the depths of 10 cm, 30 cm, 50 cm and 100 cm using conventional method. **(b)** Obtained sample of the soil column. **(c)** Core sampling augur through which the soil column was obtained, and **(d)** Schematic of the Augur system.

Comparison of traditional methods to the augur-assisted approach, reveals significant advantages. Figure 15 (**a**) depicts conventional sensor deployment through earth pits, highlighting the possibility of soil texture alteration and longer settlement times. In contrast, Figure 15 (**b, c, d**) depicts augur-assisted sensor deployment, which is a more efficient and environment friendly process. While traditional methods may take 30-45 days or longer for settlement, particularly after heavy rains, the augur has proven to cut settlement times down to one-third of the conventional soil deployment approach, making it a valuable advancement in sensor deployment technology

## c. Interfacing (Communication)

### I. Data Management:

For field-scale data collection, data archival is vital for secure and organized storage. This involves systematically saving data with timestamps for chronological tracking. Choosing the right storage medium, like non-volatile memory or external devices such as SD cards, improves data longevity and

accessibility. The logger circuit's software must have efficient data handling algorithms for managing space and easy retrieval of archived data. Regular backups and maintenance protocols safeguard against data loss. A well-designed archival system enhances the reliability and utility of the logger circuit, allowing users to derive significant insights from data analysis while maintaining data integrity.

## II. Data communication using GSM/GPRS module

The data transmitted here using the GSM/GPRS module called Sim800L module. The wireless communication is done through email using GPRS (internet) while messages are sent using the GSM feature of this module.

**Table 2:** AT commands for the data communication using GSM/GPRS module.

| Function | Command Syntax | Description | Response |
|---|---|---|---|
| **Module Initialization** | AT | Check module connectivity. | OK |
| **Signal Quality Check** | AT+CSQ | Check signal strength. | +CSQ: 20,0 |
| **Network Registration Status** | AT+CREG? | Check network registration status. | +CREG: 0,1 (Registered) |
| **GPRS Connection Type** | AT+SAPBR=3,1,"CONTYPE","GPRS" | Set GPRS connection type. | OK |
| **APN Configuration** | AT+SAPBR=3,1,"APN","internet" | Set Access Point Name (APN). | OK |
| **Activate GPRS** | AT+SAPBR=1,1 | Open bearer (activate GPRS). | OK |
| **Set SMS Format (Text Mode)** | AT+CMGF=1 | Set SMS format to text mode. | OK |
| **Send SMS Message** | AT+CMGS="+91XXXXXXXXXX" | Send SMS to a specified number. | +CMGS: 1 |
| **Read All Messages** | AT+CMGL="ALL" | List all received messages. | Message list with details |
| **Read Specific Message** | AT+CMGR=1 | Read message at position 1. | Message content and metadata |
| **Delete Specific Message** | AT+CMGD=1 | Delete message at position 1. | OK |
| **Delete All Messages** | AT+CMGDA="DEL ALL" | Delete all stored messages. | OK |
| **Check GPRS Status** | AT+CGATT? | Check if GPRS is attached. | +CGATT: 1 (Attached) |

| Function | Command Syntax | Description | Response |
|---|---|---|---|
| **Close GPRS Connection** | AT+SAPBR=0,1 | Close the bearer connection. | OK |
| **Set Email Profile** | AT+EMAILCID=1 | Set an email profile for sending. | OK |
| **Set Email Timeout** | AT+EMAILTO=30 | Set timeout to 30 seconds. | OK |
| **Configure SMTP Server** | AT+SMTPSRV="smtp.gmail.com",465 | Set SMTP server and port. | OK |
| **SMTP Authentication** | AT+SMTPAUTH=1,"username@gmail.com","password" | Configure email authentication. | OK |
| **Set Email Sender** | AT+SMTPFROM="username@gmail.com","My Device" | Define the sender's email address. | OK |
| **Define Email Recipient** | AT+SMTPRCPT=0,0,"recipient@gmail.com","Recipient Name" | Set the recipient's email address. | OK |
| **Set Email Subject** | AT+SMTPSUB="Test Email from SIM800L" | Define the subject of the email. | OK |
| **Set Email Body** | AT+SMTPBODY="This is a test email sent using the SIM800L." | Define the email content. | OK |
| **Send Email** | AT+SMTPSEND | Initiate email transmission. | +SMTPSEND: 1 |

## III. Data communication using WIFI:

The ESP32 microcontroller, equipped with a built-in Wi-Fi, which facilitates seamless wireless data transfer. To initiate this process, the necessary Wi-FI library needs to be included in the appropriate program file with network credentials. After successfully establishing a Wi-Fi connection, we can employ various protocols such as HTTP or MQTT for efficient data transfer.

**Table 3:** Commands for Data Communication Over Wireless Networks (Wi-Fi)

| Command/Function | Description | Example Usage |
|---|---|---|
| WiFi.begin(ssid, password); | Connects to a Wi-Fi network. | WiFi.begin("MySSID", "MyPassword"); |
| WiFi.status(); | Check the current Wi-Fi connection status. | if (WiFi.status() == WL_CONNECTED) |
| WiFi.disconnect(); | Disconnects from the current Wi-Fi network. | WiFi.disconnect(); |
| WiFi.localIP(); | Retrieves the local IP address. | Serial.println(WiFi.localIP()); |
| WiFi.scanNetworks(); | Scans for available Wi-Fi networks. | int n = WiFi.scanNetworks(); |
| WiFi.reconnect(); | Attempts to reconnect to the last connected network. | WiFi.reconnect(); |
| WiFi.softAP(ssid, password); | Creates a Wi-Fi Access Point (AP). | WiFi.softAP("MyAP", "APPassword"); |
| WiFi.macAddress(); | Gets the MAC address of the ESP32. | Serial.println(WiFi.macAddress()); |

**Table 4:** HTTP Protocol Commands (Using HTTP Client Library)

| Command/Function | Description | Example Usage |
|---|---|---|
| http.begin(url); | Initializes the HTTP connection. | http.begin("http://example.com/data"); |
| http.GET(); | Send an HTTP GET request. | int httpCode = http.GET(); |
| http.POST(data); | Sends an HTTP POST request with payload. | http.POST("sensor=data"); |
| http.PUT(data); | Send an HTTP PUT request. | http.PUT("update=data"); |
| http.addHeader(key, value); | Adds an HTTP header to the request. | http.addHeader("Content-Type", "application/json"); |
| http.responseText(); | Retrieves the response text from the server. | String payload = http.getString(); |
| http.errorToString(code); | Converts HTTP error code to a readable string. | Serial.println(http.errorToString(httpCode)); |
| http.end(); | Terminates the HTTP connection. | http.end(); |

**Table 5:** MQTT Protocol Commands (Using Pub Sub Client Library)

| Command/Function | Description | Example Usage |
|---|---|---|
| client.setServer(broker, port); | Sets the MQTT broker and port. | client.setServer("broker.hivemq.com", 1883); |
| client.connect(clientID); | Connects to the MQTT broker. | client.connect("ESP32Client"); |
| client.publish(topic, message); | Publishes a message to a specified topic. | client.publish("home/sensor", "25.4°C"); |
| client.subscribe(topic); | Subscribes to a specified topic. | client.subscribe("home/command"); |

| Command/Function | Description | Example Usage |
|---|---|---|
| client.loop(); | Keeps the MQTT client connected. | client.loop(); |
| client.connected(); | Checks if the client is connected to the broker. | if (client.connected()) { ... } |
| client.disconnect(); | Disconnects from the MQTT broker. | client.disconnect(); |
| client.setCallback(callback); | Sets a callback function for incoming messages. | client.setCallback(callbackFunction); |

# 3. Results

## a. Soil Sampling and the Calibration Process

The scope of point scale observation depends on the scales of interest and heterogeneity of the study area, for which the applicability is localised. Field scale measurement bridges the gap between satellite (coarse observations) and point sensors. They effectively average out heterogeneities by incorporating point observations, and widens the range of utility from hydrometeorological to agricultural applications.

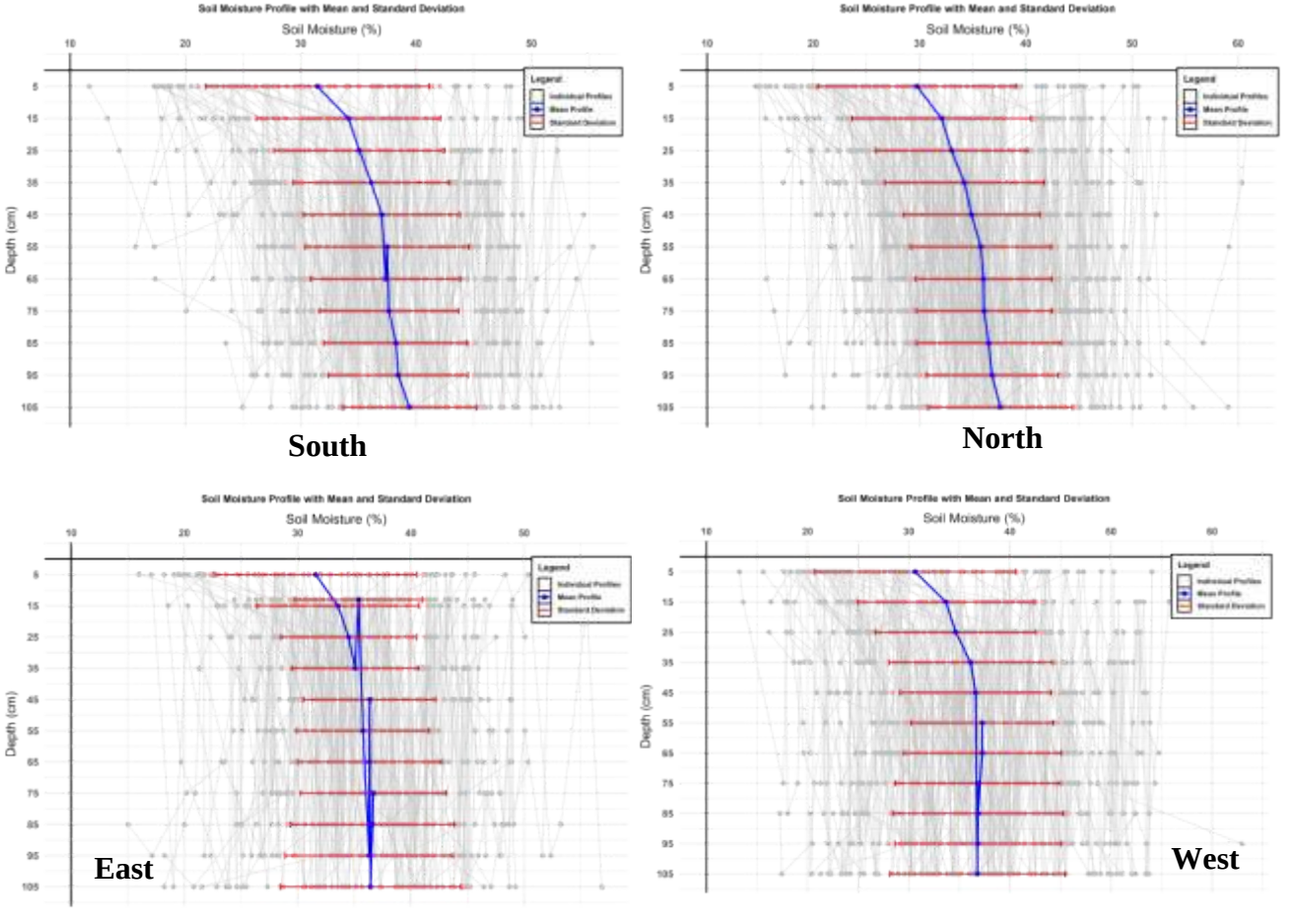


**Figure 16:** Layer by layer soil moisture observations (profile) obtained using gravimetric analysis across different quadrants (grey curves). Blue profile represents the average SM profile for all the profiles with standard deviation represented in red over the corresponding quadrant at the IITM-COSMOS site.

The first step in the soil moisture (SM) profile measurement network is to integrate diverse sensors with observational techniques. To estimate field-scale SM, a network of indigenously

assembled, low-cost capacitive SM sensors were strategically deployed, as indicated by the orange points in Figure 14(**b**). Data collected from multiple depths across various locations at the IITM-COSMOS site was systematically analyzed and compared using visualization. Figure 16 provides two distinct representations of the SM profile obtained using gravimetric method: the blue line depicts the quadrant-wise average SM profile for the site, while the grey line illustrates individual profiles recorded at different depths across multiple locations.

Determining the most accurate SM profile among these variations is a fundamental question. From the point of view of point measurements all profiles are correct, as SM variations are highly sensitive to spatial heterogeneity. Each profile reflects the unique characteristics of its specific location. Integrating these point measurements with area-averaging techniques offers a more representative of moisture distribution across the landscape. Estimating field-scale SM requires a structured approach involving sensor deployment, data collection, and appropriate averaging techniques. SM sensors are strategically positioned to capture continuous measurements of moisture content at various locations. These point-scale observations serve as the foundation for field-scale SM estimation, which is refined through systematic averaging methods. The accuracy of these estimates is validated through rigorous calibration procedures.

Calibration of SM sensors is a critical step in ensuring accurate and precise measurements. This process involves comparing sensor readings against standardized reference methods and establishing calibration points across the expected range of SM values. The observed variability in SM content across the study region is further assessed using multiple measurement techniques, including gravimetric and time-domain reflectometry (TDR) sensors such as the Acclima 315N (https://acclima.com/) and Stevens Hydra Probe. Gravimetric measurements serve as the reference standard against which the indigenously assembled sensors are calibrated.

Since July 2017, approximately 3,520 soil samples (from 320 soil profiles) have been collected and analyzed on a weekly basis using the conventional gravimetric method. Measurements were conducted at 10 cm intervals, extending to a depth of 1 meter from the surface. Collected samples were hermetically sealed in plastic bags to minimize potential moisture loss before analysis. The gravimetric analysis involved determining the initial mass of wet soil, followed by drying the samples at 100°C for 24 hours.

The final dry mass was then measured, allowing for the calculation of volumetric water content as follows:

**Gravimetric water content (g/g):**

$$\theta_g = \frac{M_{wet} - M_{dry}}{M_{dry}} \times 100 \quad (2)$$

**Volumetric water content (VWC in %):**

$$\theta_v = \theta_g \times \frac{\rho_b}{\rho_w} \quad (3)$$

where,

$\theta_v$ = Volumetric soil moisture content ($cm^3/cm^3$ or %)

$\theta_g$ = Gravimetric soil moisture content (g/g)

$\rho_b$ = Bulk density of the soil ($g/cm^3$)

$\rho_w$ = Density of water (typically 1 $g/cm^3$)

$M_{wet}$ = Mass of wet soil ($g/cm^3$)

$M_{dry}$ = Mass of Dry soil ($g/cm^3$)

The calculation of SM incorporated multiple factors, including bulk density of soil ($\rho_b$), density of water ($\rho_w$), and the measured masses of wet ($M_{wet}$) and dry ($M_{dry}$) soil. This process was meticulously repeated across diverse locations and soil types to achieve a comprehensive understanding of soil moisture variability. Table 6 presents a detailed summary of the soil properties considered in this analysis.

**Table 6:** Soil properties at IITM-COSMOS site Pune

| (https://www.acpune.in/index.php/department/soil-science-agriculture-chemistry/) | | | | |
|---|---|---|---|---|
| **Sr. No.** | **Particulars** | **Results** | **Method adopted** | **Reference** |
| **A.** | **Physical composition** | | | |
| 1 | Sand (%) | 58.5 | International pipette method | Piper (1966) |
| 2 | Silt (%) | 27.52 | International pipette | Piper (1966) |

| | | | | |
|---|---|---|---|---|
| | | | method | |
| 3 | Clay (%) | 13.98 | International pipette method | Piper (1966) |
| 4 | Textural class | Sandy clay loam | | |
| 5 | Bulk density ($gcm^{-3}$) | 1.14 | Core sampler | Richards (1968) |
| **B** | **Chemical composition** | | | |
| 1 | Organic carbon (%) | 0.82 (High) | Walkley and Black Rapid titration method | Allison (1975) |
| 2 | Calcium Carbonate (%) | 14.3 (High) | Allison and Moodie method | Allison and Moodie (1965) |
| 3 | Available Nitrogen (N, ka ha-1) | 133 (Very low) | Alkaline KMNO4 Method | Subbaiah and Asijae (1956) |
| 4 | Available Phosphorus ($P_2O_5$, kg $ha^{-1)}$ | 19 (Medium) | 0.5 N NaHCO3 Ascorbic acid | Olsen and Dean (1965) |
| 5 | Available Potassium ($K_2O$, kg $ha^{-1}$) | 122 (low) | Normal NH4 OAC flame photometer | Knudsen *et al.* (1982) |
| 6 | Soil pH (1:2.5 soil water suspension) | 8.3 (Strongly alkaline) | Potentiometric | Jackson (1973) |
| 7 | Electrical conductivity ($dSm^{-1}$) | 0.17 (Normal) | Conductometric | Jackson (1973) |
| 8 | Hydraulic conductivity | 4.8 (Normal) | Dakshinamurthy and Gupta (1967) | Dakshinamurthy and Gupta (1967) |
| **C** | **Soil Moisture Content** | | | |
| 1 | Field capacity (%) | 46 | Pressure plate apparatus | Richards (1968) |

## b. Calibration

The dataset obtained from the sensor outputs and compared with the thermogravimetric measurements of soil moisture across the investigated range (Figure 16). To calibrate the sensor system, we applied a

linear regression approach, treating the sensor's voltage output as a function of soil moisture. The resulting constant parameters from this regression served as the basis for the calibration function, specifically tailored to our local soil type—sandy clay loam.

The thermogravimetric measurements were used as a reliable reference, following standard calibration procedures. By fitting the sensor output to these reference values, we derived a best-fit model, enabling accurate estimation of volumetric water content (θ). The final calibration equation, formulated through this process, was used to convert sensor voltage readings into meaningful soil moisture values.

$$\theta = -0.0697x - 24.096 \quad (4)$$

Where θ represents volumetric water content and $x$ is an digital value.

Figure 17 shows the relationship between Gravimetric observations and the analog value of economically (low cost) assembled sensors. While the overall trend is clear, there are some differences between what the sensor records and Gravimetric observations.

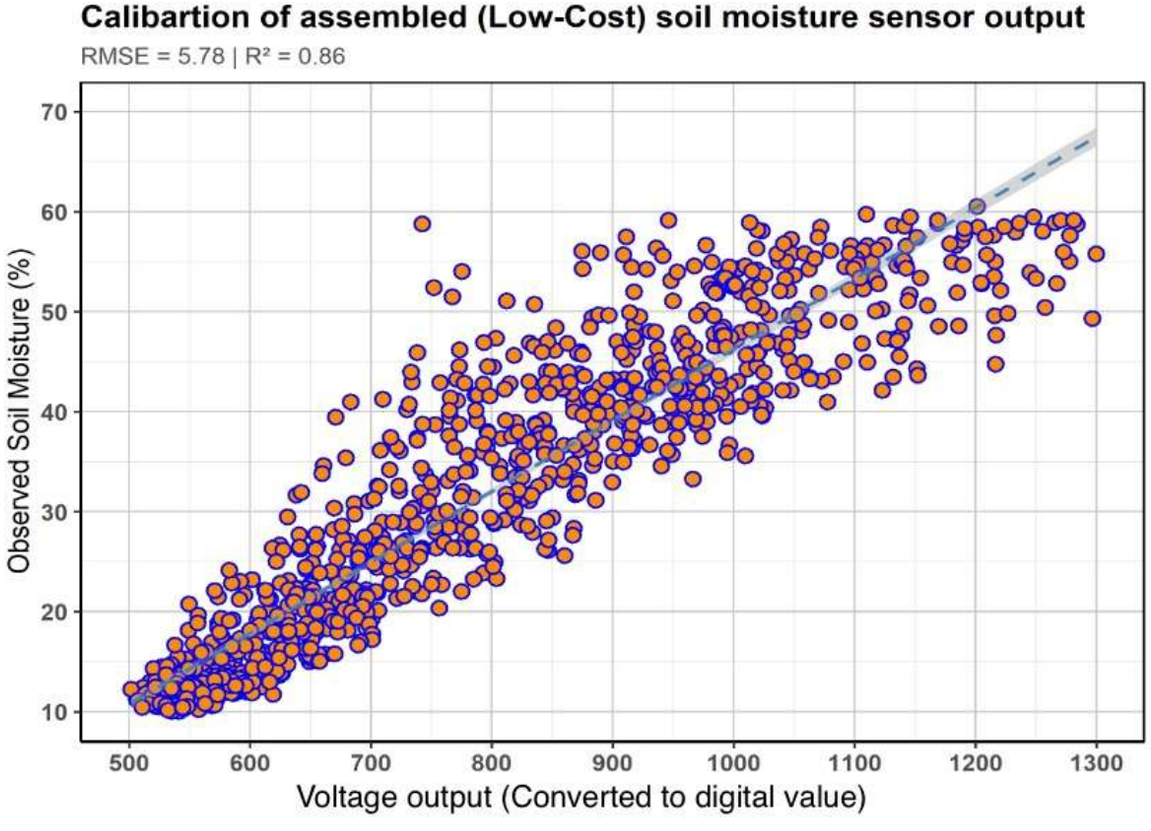


**Figure 17:** Scatter plot between voltage output (converted to digital value; see equation 1 and 4) recorded using assembled soil moisture sensor and the gravimetric observations (converted to

volumetric SM in %). The dashed line with grey shaded area represents the best fit with confidence interval respectively.

These gaps can happen for many reasons—things like changes in soil texture, how compact the soil is, temperature fluctuations, or even interference from nearby electronics or salinity in the soil. Over time, sensors can also drift ($\pm 2 - 10\%$) from their original calibration. To deal with these differences, it is important to regularly check sensor accuracy by comparing the readings to ground-truth measurements taken under different conditions. Doing this helps fine-tune the calibration and ensures the sensor continues to give reliable data, especially when things like weather, irrigation, or seasonal changes affect soil moisture. Calibration can also be tailored to specific soil types by taking into account factors like bulk density, organic matter, and mineral content.

At the IITM-COSMOS site, we applied a customized calibration for the sandy clay loam soil. The results were promising—the sensor was able to estimate soil moisture quite accurately, with $R^2$ values ranging from 0.79 to 0.86 and RMSE values between 4.9% and 5.7% across multiple depths. This shows that capacitive soil moisture sensors, when properly calibrated, can be used confidently for field monitoring and land–atmosphere studies. Also it is important to remember that real-world conditions can still affect performance. Things like temperature changes, soil salinity, and uneven soil textures can lead to differences between lab calibrations and field behaviour. Even so, lab calibration remains essential. It gives a solid baseline and helps create models that can later be tweaked for specific field conditions.

After completing the calibration, we were able to build a full field-scale dataset using the best-fit equation. The layer-by-layer soil moisture patterns from 2019 to 2021 are shown in Figure 18a, giving a detailed picture of how moisture varied across time and depth. We also looked at soil temperature, which—like moisture—needs calibration.

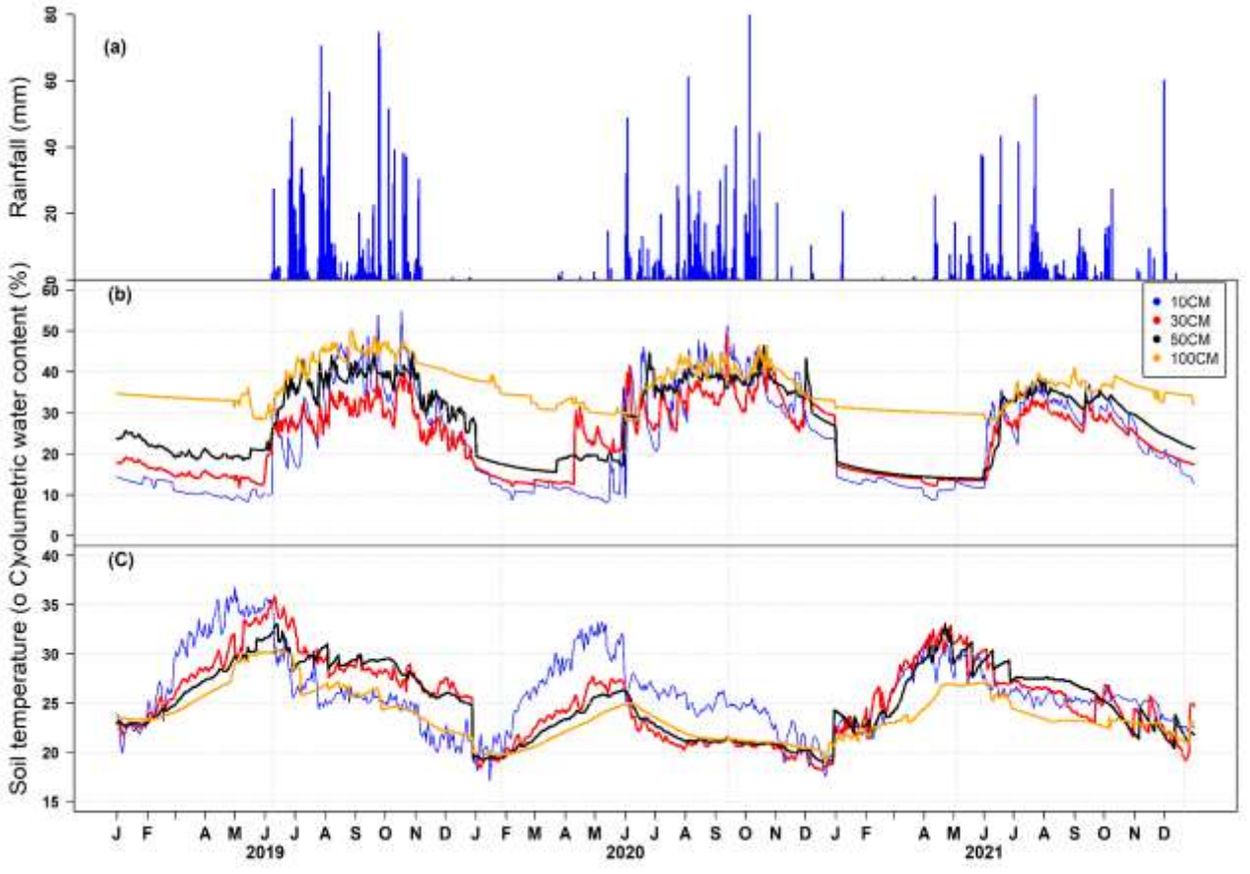


**Figure 18:** Time series of **(a)** Rainfall (mm) measured at study site, **(b)** Field scale (area averaged) soil moisture (%) and **(c)** Soil temperature (°C) at different levels: 10 cm (blue), 30 cm (red), 50 cm (black) and 100 cm (yellow) for the period 2019-2021.

To ensure accuracy, we compared the temperature sensor readings with standard temperature probes and gravimetric observations placed at the same depth across the site. The results are encouraging, with the sensor estimating soil temperature with good accuracy, achieving RMSE values ranging from 3.9% to 4.7%. By identifying and correcting for consistent errors across different soil types and weather conditions, we derived correction factors that help us monitor soil temperature more reliably over the long term. These results are presented in Figure 18b. In addition to the hydrological variables, meteorological variables such as atmospheric pressure, temperature at 2 meter height, and relative humidity) are also measured at the IITM-COSMOS site (Figure 19).

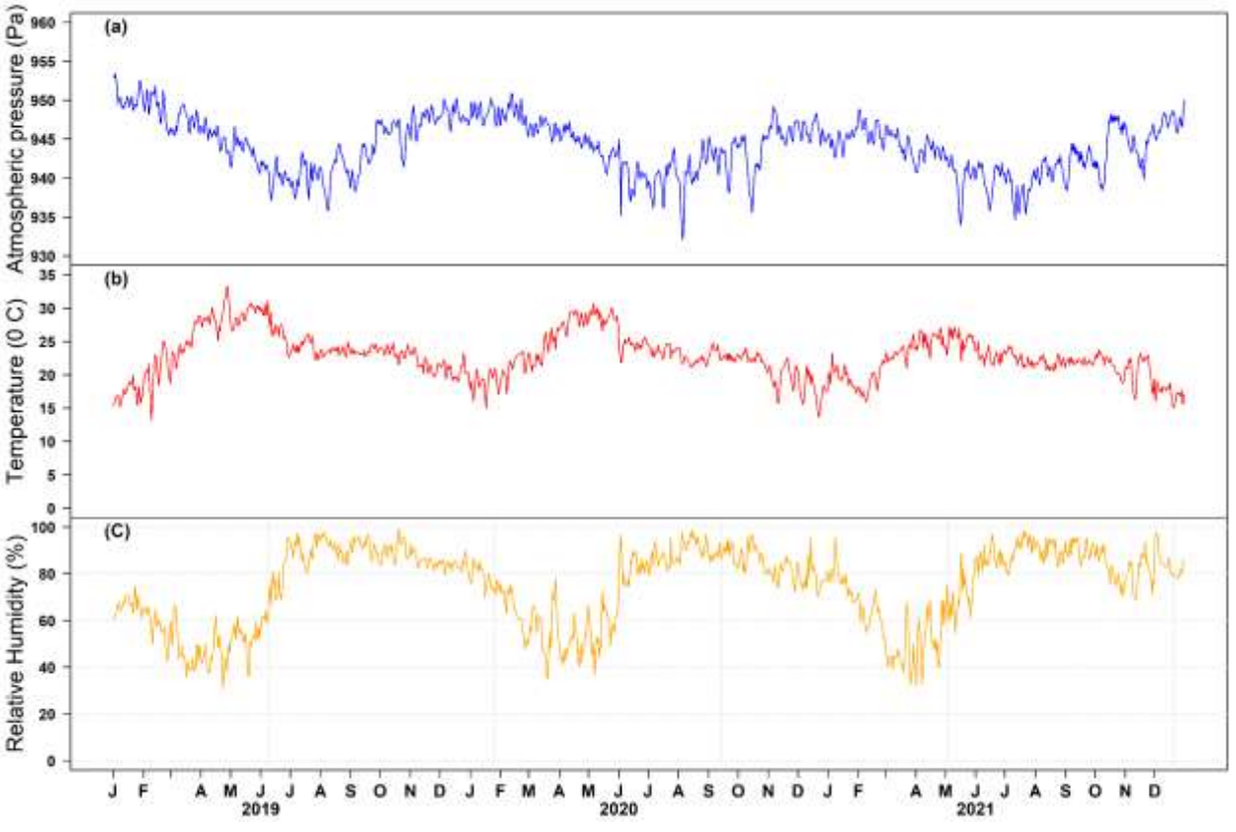


**Figure 19:** Atmospheric variables: **(a)** Atmospheric pressure, **(b)** Temperature (2-meter), and **(c)** Relative humidity, measured at IITM-COSMOS site for the period 2019-2021.

## c. Validations:

Taylor statistics (Taylor, 2005; 2001), presented in Figure 20, was employed to assess the variability of SM at the field scale. The upper panel (Figures 20 a and b) represents the comparison of surface and subsurface SM variability among various datasets (observations, reanalysis, model, and satellite) with gravimetric observations. The lower panel (Figures 20 c and d) depicts surface and sub-surface soil temperature variability.

The SM measurements due to the Assembled System, COSMOS-probe, and Hydra-Probe are found to align with gravimetric measurements and hence provide the best estimates of SM variability. Among the reanalysis and model datasets, GLDAS demonstrates comparatively better performance, with only minor deviations in variability amplitude. Satellite products (SMAP, SMOS) show lower accuracy but provide useful large-scale data. SMAP outperforms SMOS in correlation and error metrics and hence is used for comparison in this study.

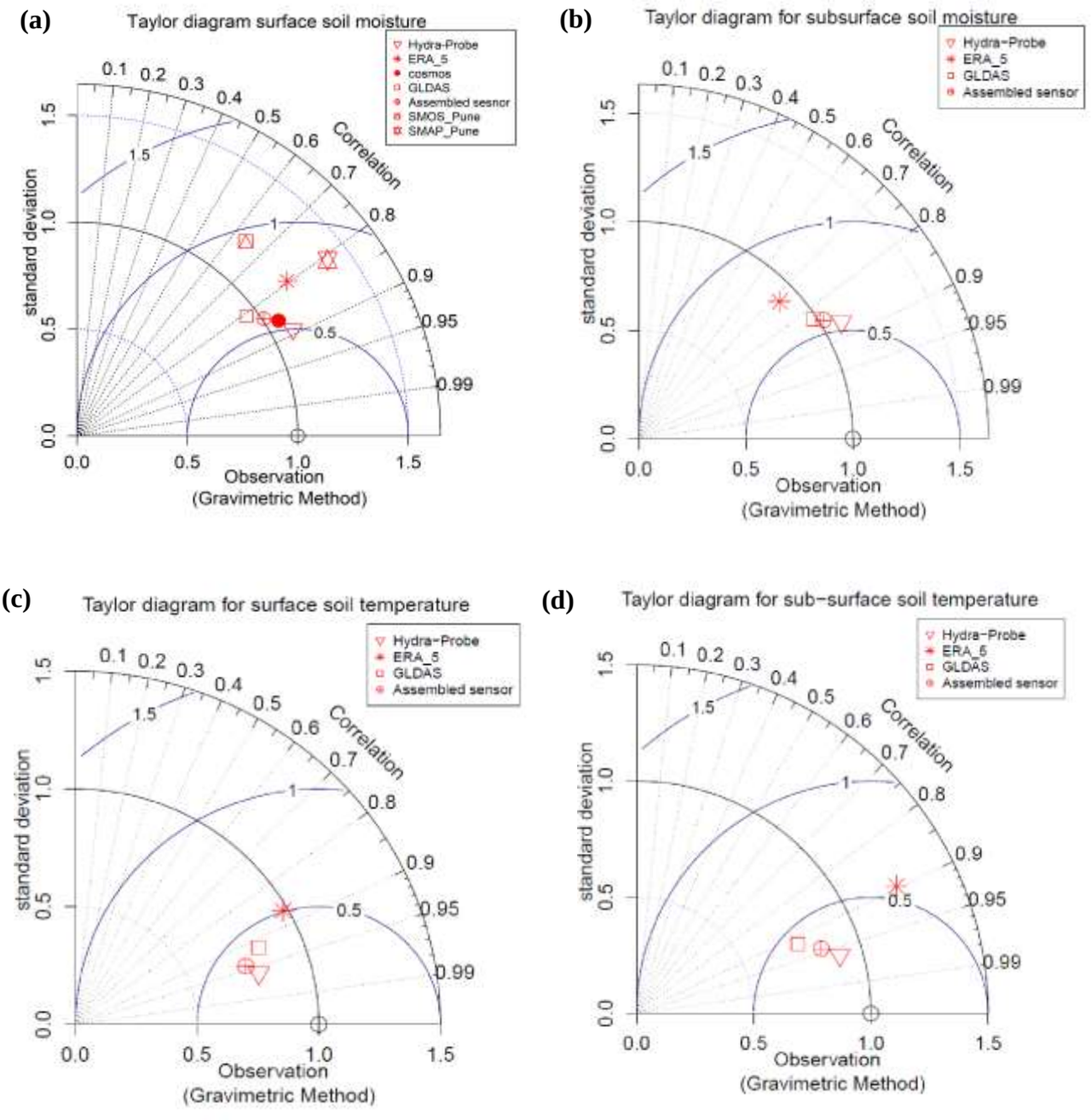


**Figure 20:** Taylor Diagram for **(a)** surface soil moisture (5 cm), **(b)** sub-surface soil moisture (100 cm), **(c)** surface soil temperature (5 cm), and **(d)** sub-surface soil temperature (100cm), for comparison with different SM data sets (Hydra Probe In-situ sensor (downward triangle), COSMOS (filled circle), Assembled (Low-cost) sensor (circle with cross), ERA 5 (star), and GLDAS (square); remote sensing Product (SMOS, SMAP) represented by distinct symbols) with validation reference to Gravimetric observation (circle on x-axis; converted to volumetric SM) collected at IITM-COSMOS site.

**Table 7:** Comparison of soil moisture statistics between gravimetric observations and model / reanalysis data products, measurements due to standard and assembled sensors. Here RMSE, STD, Mean and Bias are in m3/m3 and UbRMSE is in %.

| | | **Surface** | | | | | | | **Subsurface** | | | |
|---|---|---|---|---|---|---|---|---|---|---|---|---|
| | **Unit** | **GLDAS** | **ERA** | **Assembled sensors** | **Hydra-probe** | **COSMOS** | **SMOS** | **SMAP** | **GLDAS** | **ERA** | **assembled sensors** | **Hydra-probe** |
| **Correlation** | | 0.84 | 0.79 | 0.85 | 0.9 | 0.89 | 0.64 | 0.80 | 0.82 | 0.72 | 0.85 | 0.87 |
| **RMSE** | **($m^3/m^3$)** | 0.05 | 0.07 | 0.04 | 0.03 | 0.04 | 0.078 | 0.061 | 0.05 | 0.07 | 0.04 | 0.03 |
| **STD** | **($m^3/m^3$)** | 0.25 | 0.43 | 0.24 | 0.25 | 0.35 | 0.61 | 0.051 | 0.03 | 0.02 | 0.03 | 3.69 |
| **Mean** | **($m^3/m^3$)** | 0.19 | 0.21 | 0.18 | 0.20 | 0.16 | 0.23 | 0.21 | 0.22 | 0.24 | 0.20 | 0.21 |
| **Bias** | **($m^3/m^3$)** | 0.02 | 0.03 | 0.01 | 0.01 | 0.02 | 0.06 | 0.04 | 0.02 | 0.35 | 0.48 | 0.42 |
| **UbRMSE** | **(%)** | 3.70 | 5.76 | 3.78 | 2.57 | 2.87 | 2.6 | 3.2 | 4.96 | 7.36 | 5.10 | 3.36 |

# 4. Summary and Discussion

This report presents the development of a novel field-scale hydro-meteorological observation system at the IITM-COSMOS Pune site in India. Incorporating an IoT-based embedded system for hydro-meteorological observations marks a significant advancement in real-time climate monitoring. Meticulous deployment and calibration of hydro-meteorological sensors at the IITM-COSMOS site have produced invaluable insights into the complex dynamics of soil hydrology and land-atmosphere interactions across field-scale. Field-scale SM and ST monitoring offer substantial advantages over point-scale measurements by capturing spatial variability more accurately across larger areas. This approach enables pursuing of temporal surface and subsurface variability over longer time frames, providing insights into seasonal trends and long-term patterns. Integration of analysis of all the soil profiles facilitates a deeper understanding of hydro-meteorological processes such as precipitation, evapotranspiration, and infiltration. Moreover, field-scale SM and ST data serve as crucial inputs for hydrological models and weather forecasting systems, enhancing predictions related to soil moisture conditions, runoff, and groundwater recharge. Additionally, field-scale monitoring supports precision agriculture practices by providing detailed information about SM and ST conditions, enabling optimized irrigation, fertilization, and planting strategies.

Deployment of SM sensors at multiple depths, including innovative approaches like augur-assisted sensor deployment, minimizes soil disturbance and enhances data reliability. Integration of data communication technologies such as Bluetooth Low Energy (BLE), GSM/GPRS, and Wi-Fi enables real-time data transmission and enhances accessibility, empowering farmers and researchers with timely insights. The IoT-based hydro-meteorological observation system meticulously measures SM and ST through sensor interfacing, deployment, data generation, and wireless communication processes. Calibration and validation processes ensure accuracy and reliability, with the system showcasing a robust correlation with in-situ gravimetric data and low RMSE of approximately 4.1%. The study extends beyond soil parameters to encompass meteorological variables such as rainfall, atmospheric temperature, pressure, and relative humidity, providing a holistic understanding of environmental processes. The data generated enriches scientific knowledge and holds potential for informed policy decisions, optimizing agricultural practices, and fostering sustainable development. As methodologies continue to evolve, the pursuit of knowledge remains committed to building resilient and harmonious relationships with the environment.

# 5. Conclusion

This project led to the development of a reliable and affordable environmental observation system which can measure a variety of meteorological parameters e.g., soil moisture, temperature, rainfall, and atmospheric conditions. One of the key learnings from this work is the importance of properly calibrating and validating each sensor. By comparing the sensors with standard instruments and testing them in the field, we made sure the data collected is both accurate and trustworthy.

The system was tested in two very different environments, IITM-COSMOS in Pune and KBC-NMU in Jalgaon and it worked smoothly at both locations. These tests proved that the system is durable and stable, even in challenging outdoor conditions, and that it can handle continuous monitoring without any major issues. In terms of cost, the system is quite budget-friendly, making it a good option for schools, universities, research labs, and small-scale farmers. It uses commonly available parts, so it's easy to build, maintain, and upgrade. What's also exciting is that the system is ready for future expansion. It can be upgraded to include more sensors for measuring wind speed, solar radiation, and $CO_2$ levels, and can support the SDI-12 protocol which makes it easier to connect with a wide range of professional sensors.

Overall, through this project we have demonstrated that it is possible to build a dependable, affordable, and scalable environmental monitoring system capable of practical use.

# 6. Future scope

The future development of this environmental monitoring system holds immense potential, particularly through the integration of advanced modeling tools and a broader range of sensor technologies. One promising avenue lies in the optimization of field-scale observation networks using inputs from hydrological models, such as the HYDRUS simulation tool. HYDRUS enables detailed modeling of water, heat, and solute movement through variably saturated soils. By integrating data from such models, it becomes possible to strategically position sensors for maximum effectiveness, improve the accuracy of soil moisture and temperature predictions, and support precision irrigation and land management practices.

Another key area of future expansion is the implementation of the SDI-12 (Serial Data Interface at 1200 baud) protocol. SDI-12 is specifically designed for low-power, battery-operated sensor systems used in environmental monitoring. Its adoption will allow seamless communication between the data logger and a wide variety of commercial environmental sensors, facilitating plug-and-play compatibility and reducing the complexity of sensor integration. This standardized protocol supports multiple sensors on a single data line, which simplifies system wiring and enhances scalability for larger observation networks.

To enrich the system's environmental insight, the inclusion of additional sensors for measuring solar radiation, wind speed, wind direction, and atmospheric $CO_2$ concentration is a significant next step. Solar radiation data can provide vital information on photosynthetically active radiation and overall energy balance, which are critical for understanding plant growth and evapotranspiration. Wind speed and direction measurements contribute to assessments of microclimate conditions, dispersion of airborne particles, and evapotranspiration dynamics. Meanwhile, monitoring $CO_2$ levels in the atmosphere supports research into plant respiration, carbon cycling, and broader climate change studies. Building on these promising results, the next stage will focus on expanding the sensor network to encompass a broader range of soil types and climatic zones. This involves large-scale field campaigns which integrate gravimetric sampling with in-situ probes, and developing site-specific calibration models to further enhance accuracy and adaptability. By incorporating these advanced sensing capabilities along with hydrological modeling tools and serial data interface (SDI-12) communication, the system can evolve into a comprehensive, intelligent environmental monitoring platform. This would not only support scientific research in soil hydrology and meteorology but also

benefit practical applications in agriculture, forestry, and natural resource management by enabling data-driven decisions for sustainable land use.

**Resource statement**

Entire Python code and circuit diagram are available on reasonable request to the Director, IITM, Pune-4110 08. The usage of code and circuit diagrams should be appropriately acknowledged.

# References


1. Abdelmoneim, Ahmed A., et al. "Calibration of Low-Cost Capacitive Soil Moisture Sensors for Irrigation Management Applications." *Sensors* 25.2 (2025): 343.Allison, L. E. (1975). *Organic Carbon.* In C. A. Black (Ed.), Methods of Soil Analysis, Part 2: Chemical and Microbiological Properties (pp. 1367–1378). American Society of Agronomy, Madison, WI.

2. Allison, L. E., & Moodie, C. D. (1965). *Carbonate.* In C. A. Black (Ed.), Methods of Soil Analysis, Part 2: Chemical and Microbiological Properties (pp. 1379–1396). American Society of Agronomy, Madison, WI.

3. Bournas A, Baltas E (2023) Analysis of weather radar datasets through the implementation of gridded rainfall-runoff model. Environ Process 10:7. https://doi.org/10.1007/s40710-023-00621-2

4. Brocca, L., Ciabatta, L., Massari, C., Camici, S., & Tarpanelli, A. (2017). Soil moisture for hydrological applications: Open questions and new opportunities. *Water*, *9*(2), 140. https://doi.org/10.3390/w9020140

5. Dakshinamurthy, S., & Gupta, R. P. (1967). *A study of soil permeability under field conditions.* Journal of the Indian Society of Soil Science, 15(3), 225–231.

6. Fan, J., McConkey, B., Wang, H., and Janzen, H.: Root distribution by depth for temperate agricultural crops, Field Crop. Res., 189, 68–74, https://doi.org/10.1016/j.fcr.2016.02.013, 2016.

7. Goswami, Mangesh M., et al. "Understanding the soil water dynamics during excess and deficit rainfall conditions over the core monsoon zone of India." *Environmental Research Letters* 18.11 (2023): 114011. https://doi.org/10.1088/1748-9326/acffdf

8. Grimes, D. I. F., Pardo-Igúzquiza, E., & Bonifacio, R. (2022). Advances in hydro-meteorological data analysis for sustainable water resource management. *Hydrology and Earth System Sciences*, *26*(3), 789-805. https://doi.org/10.5194/hess-26-789-2022

9. Horowitz, P., & Hill, W. (2015). *The Art of Electronics* (3rd ed.). Cambridge University Press.

10. Huang, F., Yang, K., Chen, Y., & Tang, W. (2016). Improvements of cloud detection and impacts on long-term land surface and radiation budget over the Tibetan Plateau. Journal of Geophysical Research: Atmospheres, 121(20), 12,121–12,137. https://doi.org/10.1002/2016JD025496

11. Ingale, M., Singh, B. B., Mujumdar, M., Goswami, M., Ganeshi, N., Aju, C. D., Krishnan, R., & Ravichandran, M. (2025). Persistence in Physical Systems: An Application to Soil Moisture Memory. Phys. Rev. Lett., 135(16), 164201. https://doi.org/10.1103/djz5-2lsn

12. Jackson, M. L. (1973). *Soil Chemical Analysis.* Prentice Hall, New Delhi.

13. Jobbágy, Esteban G., and Robert B. Jackson. "The vertical distribution of soil organic carbon and its relation to climate and vegetation." *Ecological applications* 10.2 (2000): 423-436.

14. Knudsen, D., Peterson, G. A., & Pratt, P. F. (1982). *Lithium, sodium, and potassium.* In A. L. Page (Ed.), Methods of Soil Analysis, Part 2: Chemical and Microbiological Properties (pp. 225–246). American Society of Agronomy, Madison, WI.

15. Koster, R. D., Dirmeyer, P. A., Guo, Z., Bonan, G., Chan, E., Cox, P., ... & Yamada, T. (2004). Regions of strong coupling between soil moisture and precipitation. *Science, 305*(5687), 1138-1140. https://doi.org/10.1126/science.1100217

16. Krüger, R., Karrasch, P., and Eltner, A.: Calibrating low-cost rain gauge sensors for their applications in Internet of Things (IoT) infrastructures to densify environmental monitoring networks, Geosci. Instrum. Method. Data Syst., 13, 163–176, https://doi.org/10.5194/gi-13-163-2024, 2024.

17. Lyons, R. G. (2011). *Understanding Digital Signal Processing* (3rd ed.). Prentice Hall.

18. Mujumdar, M., Goswami, M. M., Morrison, R., Evans, J. G., Ganeshi, N., Sabade, S. S., … Patil, S. N. (2021). A study of field-scale soil moisture variability using the COsmic-ray Soil Moisture Observing System (COSMOS) at IITM Pune site. Journal of Hydrology, 597(September 2020), 126102. https://doi.org/10.1016/j.jhydrol.2021.126102

19. Ochoa-Rodriguez, S., Wang, L. P., Gires, A., Pina, R. D., Reinoso-Rondinel, R., Bruni, G., ... & Onof, C. (2019). Impact of spatial and temporal resolution of rainfall inputs on urban hydrodynamic modelling outputs: A multi-catchment investigation. *Journal of Hydrology, 573*, 554-568. https://doi.org/10.1016/j.jhydrol.2019.03.046

20. Olsen, S. R., & Dean, L. A. (1965). *Phosphorus.* In C. A. Black (Ed.), Methods of Soil Analysis, Part 2: Chemical and Microbiological Properties (pp. 1035–1049). American Society of Agronomy, Madison, WI.

21. Piper, C. S. (1966). *Soil and Plant Analysis.* Hans Publishers, Bombay, India.

22. P.K. Rajani, Guruprasad Deshpande, Mangesh Goswami, Jayesh Kolhe, Vishal Khandagale, Milind Mujumdar, Bhupendra Bahadur Singh, "IoT-Based Low-Cost Soil Moisture and Soil Temperature Monitoring System," *SSRG International Journal of Electrical and Electronics Engineering*, vol. 10, no. 10, pp. 66-74, 2023.

23. Ramesh Saha, Biswas, S., Sarmah, S. *et al.* A Working Prototype Using DS18B20 Temperature Sensor and Arduino for Health Monitoring. *SN COMPUT. SCI.* 2, 33 (2021). https://doi.org/10.1007/s42979-020-00434-2

24. Richards, L. A. (1968). *Diagnosis and Improvement of Saline and Alkali Soils.* USDA Agriculture Handbook No. 60, U.S. Department of Agriculture, Washington, D.C.

25. Saha, H., Roy, N., Nath, R. K., Saha, J., & Sadhu, P. (2020). Internet of Things for smart temperature monitoring: A review. *Journal of Ambient Intelligence and Humanized Computing, 11*(11), 4531–4556. https://doi.org/10.1007/s12652-019-01416-5

26. Segovia-Cardozo, D.A.; Bernal-Basurco, C.; Rodríguez-Sinobas, L. Tipping Bucket Rain Gauges in Hydrological Research: Summary on Measurement Uncertainties, Calibration, and Error Reduction Strategies. *Sensors* 2023, *23*, 5385. https://doi.org/10.3390/s23125385

27. Seneviratne, S. I., Corti, T., Davin, E. L., Hirschi, M., Jaeger, E. B., Lehner, I., ... & Teuling, A. J. (2010). Investigating soil moisture–climate interactions in a changing climate: A review. *Earth-Science Reviews*, *99*(3-4), 125-161. https://doi.org/10.1016/j.earscirev.2010.02.004

28. Stefanos, X., Papadopoulos, A., & Kalaitzoglou, I. (2020). Integration of UAV and ground-based sensor networks for real-time soil moisture and temperature monitoring. *Remote Sensing, 12*(14), 2289. https://doi.org/10.3390/rs12142289

29. Stewart, J. I. (2014). Hydrology in practice: Understanding water availability and climate dynamics. *Cambridge University Press*.

30. Subbaiah, B. V., & Asija, G. L. (1956). A rapid procedure for the estimation of available nitrogen in soils. *Current Science*, 25(8), 259–260.

31. Taylor, K. E. (2001). Summarizing multiple aspects of model performance in a single diagram. *Journal of geophysical research: atmospheres*, *106*(D7), 7183-7192.

32. Whan, K., Zwiers, F., Sillmann, J., & Zhang, X. (2015). The influence of soil moisture on temperature extremes in observational and modeling analyses. *Climate Dynamics, 45*(7-8), 2001-2021. https://doi.org/10.1007/s00382-014-2433-7

33. Zhang, X. (2004). Sensitivity of climate variability to land surface processes: A review. *Journal of Climate Research*, *27*(1), 1-15.

34. Zhenzhou, W., Li, J., & Wang, Y. (2018). Satellite-based monitoring of soil moisture dynamics using multi-sensor data fusion techniques. *Journal of Hydrometeorology, 19*(3), 573-590. https://doi.org/10.1175/JHM-D-17-0156.1